HHS Public Access

Author manuscript

Neuropharmacology. Author manuscript; available in PMC 2023 March 15.

Published in final edited form as:

Neuropharmacology. 2023 March 15; 226: 109409. doi:10.1016/j.neuropharm.2022.109409.

Microbial glutamate metabolism predicts intravenous cocaine self-administration in diversity outbred mice

Thi Dong Binh Tran[a], **Hoan Nguyen**[a], **Erica Sodergren**[a], **Center for Systems Neurogenetics of Addiction**[b], **Price E. Dickson**[c], **Susan N. Wright**[d], **Vivek M. Philip**[b], **George M. Weinstock**[a], **Elissa J. Chesler**[b], **Yanjiao Zhou**[e], **Jason A. Bubier**[b,*]

[a]The Jackson Laboratory Genomic Medicine, 10 Discovery Way, Farmington, CT, USA

[b]The Jackson Laboratory Mammalian Genetics, 600 Main St, Bar Harbor, ME, USA

[c]Department of Biomedical Sciences, Joan C. Edwards School of Medicine Marshall University, Huntington, WV, USA

[d]Division of Neuroscience and Behavior, National Institute on Drug Abuse, National Institutes of Health, Three White Flint North, Room 08C08 MSC 6018, Bethesda, MD, 20892, USA

[e]Department of Medicine, University of Connecticut Health Center, 263 Farmington Avenue, Farmington, CT, USA

Abstract

The gut microbiome is thought to play a critical role in the onset and development of psychiatric disorders, including depression and substance use disorder (SUD). To test the hypothesis that the microbiome affects addiction predisposing behaviors and cocaine intravenous self-administration (IVSA) and to identify specific microbes involved in the relationship, we performed 16S rRNA gene sequencing on feces from 228 diversity outbred mice. Twelve open field measures, two light-dark assay measures, one hole board and novelty place preference measure significantly differed between mice that acquired cocaine IVSA (ACQ) and those that failed to acquire IVSA (FACQ). We found that ACQ mice are more active and exploratory and display decreased fear than FACQ mice. The microbial abundances that differentiated ACQ from FACQ mice were an

*Corresponding author. Jason.Bubier@jax.org (J.A. Bubier).

Declaration of competing interest

The authors declare that they have no known competing financial interests or personal relationships that could have appeared to influence the work reported in this paper.

Credit author contribution statement

Thi Dong Binh Tran: Methodology, Formal analysis, Data curation, Investigation, Writing – original draft, Writing – review & editing, Visualization, Hoan Nguyen: Formal analysis, Data curation, Investigation, Erica Sodergren: Project administration, Investigation, Center for Systems Neurogenetics of Addiction: Conceptualization, Methodology, Investigation, Formal analysis, Data curation, Price E Dickson: Methodology, Investigation, Supervision, Writing – review & editing, Susan N Wright: Writing – review & editing, Vivek M Philip: Methodology, Conceptualization, Investigation, Formal analysis, Data curation, Writing – review & editing, George M. Weinstock: Methodology, Conceptualization, Writing – original draft, Writing – review & editing, Project administration, Funding acquisition, Elissa J Chesler: Conceptualization, Writing – review & editing, Project administration, Funding acquisition, Yanjiao Zhou: Conceptualization, Writing – original draft, Writing – review & editing, Funding acquisition, Jason A. Bubier: Conceptualization, Writing – original draft, Writing – review & editing, Project administration, Funding acquisition.

Appendix A. Supplementary data

Supplementary data to this article can be found online at https://doi.org/10.1016/j.neuropharm.2022.109409.

increased abundance of *Barnesiella*, *Ruminococcus*, and *Robinsoniella* and decreased *Clostridium IV* in ACQ mice. There was a sex-specific correlation between ACQ and microbial abundance, a reduced Lactobacillus abundance in ACQ male mice, and a decreased *Blautia* abundance in female ACQ mice. The abundance of *Robinsoniella* was correlated, and *Clostridium IV* inversely correlated with the number of doses of cocaine self-administered during acquisition. Functional analysis of the microbiome composition of a subset of mice suggested that gut-brain modules encoding glutamate metabolism genes are associated with the propensity to self-administer cocaine. These findings establish associations between the microbiome composition and glutamate metabolic potential and the ability to acquire cocaine IVSA thus indicating the potential translational impact of targeting the gut microbiome or microbial metabolites for treatment of SUD.

This article is part of the Special Issue on “Microbiome & the Brain: Mechanisms & Maladies”.

Keywords

Microbiome; IVSA; Novelty; Diversity outbred; Cocaine; Behavior; Sex differences

1. Introduction

Substance use disorder (SUD) is a chronic brain disease characterized by compulsive drug seeking and use, despite negative consequences (American Psychiatric Association. And American Psychiatric Association. DSM-5 Task Force., 2013). While candidate genes and genome-wide association study (GWAS) yield important insight into the genetic variation influencing addiction, little is known about the impact of the gut microbiome. There is growing awareness in the medical community that an imbalance of the gut microbiome (dysbiosis) is associated with various local and systemic diseases (Shreiner et al., 2015), including psychiatric disorders (Chen et al., 2021; Valles-Colomer et al., 2019; Yang et al., 2020). Dysbiosis has been reported in individuals with SUDs of various etiology, including alcohol (Day and Kumamoto, 2022), opioid (Jalodia et al., 2022), methamphetamines (Cook et al., 2019), and cocaine (Volpe et al., 2014). Furthermore, the gut microbiome can affect behavioral response to cocaine in mice (Kiraly et al., 2016). Mice treated with non-absorbable antibiotics exhibited enhanced sensitivity to cocaine reward and enhanced sensitivity to the locomotor sensitizing effects of repeated cocaine administration (Kiraly et al., 2016).

Anxiety and depression are common comorbidities of SUD (Ahmad et al., 2001). Alterations in the gut microbiome can induce anxiety and depressive-like behavior in mice, with the exact underlying mechanism remaining elusive. Metabolites, specifically short-chain fatty acids (SCFA) produced by bacterial fermentation of non-digestible carbohydrates, are important mediators in gut-brain crosstalk. Fifty percent of the body’s dopamine and upwards of 90% of the body’s serotonin are produced in the intestinal tract (Yano et al., 2015). Although these two addiction-related neurotransmitters do not directly cross the blood-brain barrier (BBB), they may affect the brain’s reward centers through immune signaling or direct interaction with the vagus nerve, resulting in neuroinflammation (Muller et al., 2020; O’Donnell et al., 2020). Administration of probiotic *Lactobacillus*

plantarum PS128 increased levels of serotonin and dopamine in the striatum and resulted in changes in anxiety-like behaviors in mice (Liu et al., 2016). Further, dysbiosis is observed in multiple psychiatric disorders including autism spectrum disorder (ASD) (Alamoudi et al., 2022). The role of *Lactobacillus reuteri* in social behavioral defects was differentiated from the *Cntnap2*-dependent control of hyperactivity in mice (Buffington et al., 2021). Subsequent metabolomic studies of *Lactobacillus reuteri* inoculation showed biopterin rescues social interaction-induced synaptic transmission (as does cocaine) through stimulation of the vagus nerve (Shiraki et al., 1996) and oxytocin release (Ciosek and Guzek, 1992; Ciosek et al., 1992). Together, these observations have resulted in translational advances, including clinical trials of microbiota-based interventions in ASD (Stewart Campbell et al., 2022). The potential of targeting the brain through the gut to address various neuropathology is becoming a reality (Cryan and Mazmanian, 2022). However, the relevant microbes, microbial molecules, and mechanisms of their action on behavior need to be identified. Mouse genetics provide a powerful and holistic approach for the detection of such targetable mechanisms of gut-behavior interaction.

The Collaborative Cross (CC) (Bubier et al., 2020) is a panel of recombinant inbred strains of mice derived from a cross of eight parental inbred lines (five classic inbred strains and three wild-derived inbred strains) (Chesler et al., 2008; Churchill et al., 2004; Saul et al., 2019; Threadgill and Churchill, 2012). These strains have been used to identify divergent responses to cocaine (Schoenrock et al., 2020). The Diversity Outbred (DO) mice were derived from CC mice outcrossed to maintain the distribution of alleles from across the eight parental strains in a unique combination in each mouse (Chesler et al., 2016; Saul et al., 2019; Svenson et al., 2012). Each DO mouse is unique, and the population is heterogeneous, giving theoretically unlimited precision in genetic mapping to identify the source of variation in complex traits. The DO harbors variation in virtually all genes and pathways in the mouse, with 45 million variants segregating. By controlling for environmental conditions known to strongly influence the microbiome (diet, water, bedding, etc.), we can narrow in on the host genetic factors that influence microbiome composition using DO mice (Bubier et al., 2021). Indeed, DO mice raised in controlled conditions have endogenous variance in their microbiome and their response to drugs associated with SUD. In a small cohort of DO mice, we previously showed that various novelty behavior measures positively correlate with multiple cocaine intravenous self-administration behavior (IVSA) metrics (Dickson et al., 2015). IVSA of cocaine is considered the gold standard methodology to model volitional drug use in rodent studies (Mello and Negus, 1996). The propensity to self-administer addictive drugs has been repeatedly associated with predisposing traits including impulsivity and novelty-seeking behaviors (Belin and Deroche-Gamonet, 2012; Cervantes et al., 2013; Flagel et al., 2014), allowing powerful assessment of the predisposing biological characteristics predictive of SUDs and related rodent phenotypes.

To correlate novelty-related behaviors with microbial composition and microbiome metabolic pathways, we examined DO mice in open field assays, light-dark assays, holeboard assays, and novelty place preference assays. Each of these assays likely represents phenotypically distinct and genetically independent constructs (Kliethermes and Crabbe, 2006). After observing mice in these four behavioral tests, gut microbiome samples were collected, then mice were subjected to cocaine IVSA testing. We compared the microbiome

of mice that acquired IVSA (ACQ) to those that failed to acquire IVSA (FACQ) and related those microbes to the naïve novelty behaviors. Finally, we explored the pathways that are predicted to differ between these groups using PICRUSt and Gut-Brain Module analysis of mWGS data.

2. Methods and materials

2.1. Animals

1,065 DO mice were evaluated in behavioral phenotyping assays including IVSA as part of a genetic mapping study led by The Center for Systems Neurogenetics of Addiction. A subset of those mice underwent microbiome analysis and are the subject of this report. For microbiome analysis, 228 J:DO (The Jackson Laboratory JR009376) from both sexes (M = 121, F = 107), spanning generations G21, G22 and G23, were purchased from the Jackson Laboratory. The mice were produced in room G200, a high barrier Pathogen & Opportunistic-Free Animal Room (Health report https://www.jax.org/-/media/jaxweb/health-reports/g200.pdf?la=en&hash=7AD522E82FA7C6D614A11EFB82547476157F00E1) and transferred at wean to an intermediate barrier specific pathogen-free room (https://www.jax.org/-/media/jaxweb/health-reports/g3b.pdf?la=en&hash=914216EE4F44ADC1585F1EF219CC7F631F881773).

Same-sex siblings were co-housed with a combined body weight of up to 15 g per side of the duplex cage at 3–5 weeks. Mice were individually housed starting at six weeks of age with a minimum of 5 days before testing. Mice were housed under (12:12) light-dark cycle and allowed *ad libitum* access to standard rodent chow [sterilized NIH31 5K52 6% fat chow (LabDiet/PMI Nutrition, St. Louis)] and acidified water (pH 2.5–3.0) supplemented with Vitamin K. JAX began supplementing the water with vitamin K in 1967 based on the results of an investigation into hemorrhagic diathesis (bleeding) sporadically noted in male mice of certain strains. Studies conducted by JAX at that time determined that low levels of vitamin K in the diet post autoclave was likely responsible for the bleeding disorder. Mice were housed in duplex, individually-vented Thoren cage #3 cages with pine-shaving bedding (Hancock Lumber) and environmental enrichment consisting of a nestlet and Shepard's shack. The mice were identified by ear notching at 3–4 weeks of age and moved between cages and testing arenas using metal forceps. Clean housing was provided through a cage change once a week. If this fell on a testing day, the mice were moved to their new, clean cage post-testing. The Jackson Laboratory follows husbandry practices in accordance with the American Association for the Accreditation of Laboratory Animal Care (AAALAC), and all work was done with the approval of our Institutional Animal Care and Use Committee (Approval #10007).

2.2. Phenotyping

At three to six months, mice were phenotyped using the open-field, light-dark, holeboard, and novelty place preference assays daily from Monday to Thursday four separate times. After novelty testing, mice underwent jugular catheter implantation surgery to prepare for cocaine intravenous self-administration (IVSA). Complete phenotyping details can be found at https://phenome.jax.org/projects/CSNA03/protocol

2.2.1. Open field apparatus—A square-shaped, clear polycarbonate arena (Med-Associates #MED-OFAS-515U) with dimensions 17.5 inches length × 17.5 inches width × 10.0 inches height (44.5 cm × 44.5 cm × 25.4 cm) was used for the open field arena. External to the arena's perimeter at the floor level, on the left and right sides, were a pair of horizontal infrared photobeam sensors (16 × 16 beam array). An additional pair of infrared photobeam sensors raised 3 inches from the arena floor (16 × 16 array) were situated at the front and rear external sides of the arena and used to capture vertical activity. Each arena was placed within a sound attenuated, ventilated cabinet with interior dimensions: of 26′′W × 20′′H × 22′′D (Med Associates, #MED-OFA-017). Each cabinet contained two incandescent lights, each affixed in the upper rear two corners of the cabinet at the height of approximately 18.5 inches from the center of the arena floor, providing illumination of 60 ± 10 lux when measured in the center of the arena floor. Data was collected using Activity Monitor software:7.0.5.10 SOF-812 (Med Associates, Inc; RRID:SCR_014296). For all behavioral assays, mice were transported from the housing room to the procedure room on a wheeled rack and left undisturbed to acclimate to the anteroom adjacent to the procedure room for a minimum of 30 min. Before the first mouse was placed into any arena and between subjects, the chamber was thoroughly sanitized with 70% ETOH solution (in water), and the box was wiped dry with clean paper towels. After all testing for the day, the subjects were returned to the housing room, and the arenas were sanitized with Virkon followed by 70% ETOH to remove any Virkon residue.

2.2.1.1. Open field activity.: At the start of each testing session, after the mice were acclimated to the anteroom for 30 min, the mice were individually placed in the center of the arena, facing the rear of the chamber. The lid was placed atop the arena, and the chamber door was closed. The tracking software detects the mouse in the arena and starts automatically. The tracking software automatically ends the tracking for the subject 60 min after the mouse was initially detected by the software. Numerous metrics were recorded for each mouse (see data definition Sup Table 1).

2.2.1.2. Light-dark.: A black polycarbonate insert that does not interrupt infrared beams (Med Associates) was placed into the back half of the open field arena, with the entry door opening toward the arena's front center, thereby reducing the light levels within the dark side of the box. At the start of each testing session, mice were individually placed in the center of the arena, on the light side, facing the rear of the chamber (facing the dark Side). The lid was placed atop the arena, and the chamber door was closed. The tracking software detected the mouse in the arena and started automatically. The tracking software automatically ends the tracking for the subject 20 min after the mouse was initially detected by the software. Numerous metrics were recorded for each mouse (see data definition Sup Table 1).

2.2.1.3. Holeboard.: The holeboard floor (Med Associates) was inserted into the open field arena. The holeboard floor consists of two components: the metal floor—with which the mice were in contact—was comprised of 16 evenly spaced holes, and the under plate contains 16 holes matching those on the metal plate with wire mesh for baiting the holes. At the start of each testing session, subjects were individually placed in the center of the arena, facing the rear of the chamber. The lid was placed atop the arena, and the chamber door was

closed. The tracking software detected the mouse in the arena and started automatically. The tracking software automatically ended the tracking for the subject 20 min after the mouse was initially detected by the software. Numerous metrics were recorded for each mouse (see data definition Sup Table 1).

2.2.2. Novelty place preference—The Novelty Place Preference apparatus is a rectangular shaped, three-chambered arena (acrylic or polycarbonate materials) with dimensions (white/black chambers: 5 in length, 6.5 in width, 5 in height; grey center chamber: 5 in length, 3.5 in width, 5 in height) with automatic doors between the three sections, and a clear, aerated lid (Med Associates, Inc.) The bottom of the arena contained pairs of horizontal infrared photobeam sensors at the floor level, which were not visible to the mouse. Each arena was placed within a sound attenuated, ventilated cabinet with dimensions 25 in width × 26 in depth × 21 in height (Med Associates, Inc.) Before the start of testing, upon transport to the procedure room, subjects were briefly handled and assessed for welfare concerns that may have resulted in exclusion from testing (e.g., fight wounds or bite marks). They were then left undisturbed to acclimate to the procedure room environment for a minimum of 60 min before testing began. The mouse was placed in the center grey chamber, and all hinged ceiling doors were closed. Once the software detected the placement of the mouse, the ceiling light in the chamber was turned off, and a 5-min acclimation timer was started. After the 5-min acclimation period, the motorized guillotine doors leading to the preassigned exposure chamber (black or white) opened, and the ceiling lights turned on. After 20 min, the exposure session was complete; the guillotine door closes. Immediately upon the conclusion of the exposure program, the mouse was placed back into the center compartment. If a mouse was in the center chamber after the exposure program as above, the mouse was handled and removed from the center chamber and then replaced in the center chamber to mirror the handling of all subjects between exposure and test programs. Upon all subjects being returned to the program, the ceiling light in the chamber turned off, and a 5-min acclimation timer started. After the 5-min acclimation period, *both* motorized guillotine doors leading to the black and white chambers opened, and the ceiling lights turned on. A 10-min testing timer begin. After 10 min, the session was complete, and the doors closed. Only one metric was recorded: the % movement on the novel side.

2.3. Fecal collection

After the four days of behavioral testing, fecal pellets were collected from the mice before surgery on day five. Mice were placed in a clean wean pen for 5 min. Any fecal pellets deposited were immediately collected, placed in Eppendorf tubes, and stored at −80 °C until DNA extraction.

2.4. Cocaine intravenous self-administration (IVSA)

Mice were tested following a modification of the protocol described in Dickson et al. (2015). Mice >12 weeks of age underwent indwelling jugular vein catheterization under oxygen/isoflurane anesthesia by The Jackson Laboratory surgical services. The catheter (Instech, C20PU-MJV, Plymouth Meeting, PA) was routed through the stainless coupler of a mesh button. The mesh button was sutured in place subcutaneously. The port was flushed with

saline and filled with 10 μl of lock solution (Lumen lock solution; 500 IU heparin/ml lock solution). The catheter was capped with a protective aluminum cap (Instech., PHM-VAB95CAP). The mouse was observed for at least three days after surgery to ensure the incision was healing properly. If mice exhibited pain signs, buprenorphine (0.05 mg/kg SQ) was administered every 4–5 h or carprofen (5 mg/kg SQ) was administered every 24 h. Mice were provided a minimum ten-day post-operative recovery period in their home cage before testing. Mice were transported in their home cages from the housing room to the procedure room on a wheeled transport rack. Before the start of testing, upon transport to the procedure room, mice were weighed (once a week) and briefly handled to be assessed for any welfare concerns that may result in exclusion from testing (e.g., wounds or looking sickly). IVSA data were collected using Med Associates operant conditioning chambers (307 W), fitted with two retractable levers on the front wall flanking the right and left sides of the center panel food hopper. Directly over each lever (~2–3 inches above) were red stimulus lights. A house light (ENV-315 W) was centrally mounted on the rear wall. A modified Plexiglas floor, fabricated at the Jackson Laboratory, was fitted to cover the metal floor grids. The chambers were within sound attenuating cubicles (ENV-022MD). A 25-gauge single-channel stainless steel swivel was mounted to a counterbalanced lever arm attached to the outside of the chamber. Tubing was used to connect a syringe mounted on the infusion pump to the swivel and to connect the swivel to a vascular access harness. Operant conditioning chambers were controlled by a Med Associates control unit using MED-PC IV software (RRID:SCR_012156).

Mice began cocaine IVSA testing on a fixed-ratio 1 (FR1) schedule at a dose of 1.0 mg/kg/infusion of cocaine hydrochloride (NIDA Drug Supply). Infusions from the active lever were at 8.85 μl/sec, with 1 s per 10 g mouse weight. Each IVSA session was 2 h each day. After each day of testing, Baytril (enrofloxacin) was administered by catheter to the mice at 22.7 mg/kg, followed by a 20 μl injection of Heparin lock solution (100 U/ml heparin/saline). Acquisition criteria were met when mice had 5 (could be non-consecutive) sessions with ≥10 infusions. Mice were excluded from the study if they did not acquire within 18 days of starting. A mouse may be excluded earlier if it can’t meet the acquisition criteria within 18 days. The mouse reached stabilization when the number of infusions didn’t vary more than 20% for the last two consecutive sessions. Following stabilization, the mice were tested on 1.0 mg/kg through a dose-response curve from high to low doses. During this testing phase, the mice were assessed for self-administration response across a 4-dose cocaine dose-response curve (DRC). Doses were presented in the following order: 1.0, 0.32, 0.1, 0.032 mg/kg/infusion. Mice were tested on consecutive days on the same dose until stabilization criteria were met or a max of 5 sessions, then moved on to the next dose. Following the DRC, mice were evaluated for extinction, defined as a reduction in lever presses on the active lever that does not result in a cocaine infusion reward. During extinction sessions, subjects were connected to saline-filled infusion tubing; however, the infusion pump was not activated. During extinction sessions, the house light was continuously illuminated, stimulus lights were never illuminated, and lever presses have no programmed consequences. Mice were tested for 3–9 days, depending on whether the extinction criteria are met. The number of active lever presses on the first day of the extinction session was the reference baseline for establishing extinction. The criteria for extinction were defined as follows: a) When active

lever presses are reduced to <50% of the established baseline from the initial extinction session; and b) the variance of the final two days is within 20% of the established baseline from the initial extinction session; c) if active lever presses are <10 on or after day 3. Subjects not reaching extinction criteria within nine days were advanced to the reinstatement stage. Following extinction, responding on the active and inactive levers was examined for two daily 2-h sessions. During reinstatement sessions, as in the acquisition and DRC, drug-paired stimuli, including the sound of the infusion pump, were presented; however, there was no infusion into the mouse. Specifically, mice were connected to infusion tubing, which was connected to a sterile-saline-filled syringe, but the syringe was not in the pump. Thus, mice do not receive drug infusions. Initiation of lever pressing was due to conditioned stimuli. Numerous metrics were recorded; see data definition Supp Table 1. Not all mice that entered the study completed it. Mice may fail to survive the surgery, have a non-patent catheter, a systemic infection, a local infection at the catheter port, cocaine overdose, or air embolism. These mice were excluded from the study.

2.5. 16S rRNA gene sequencing, data processing and microbiome functional prediction

Shoreline Complete V1V3 kit (Shoreline Biome, cat #SCV13) https://www.shorelinebiome.com/product/v1-v3-16s-amplicon-kit/) was used per manufacturer's instructions for DNA extraction, library preparation and sequencing. Briefly, ~5 mg of mouse fecal pellet was lysed with a combination of heat, pH, and cell wall disruptors in a single step. DNA was recovered using the supplied magnetic beads, and an aliquot from each sample was transferred to a well in the provided PCR plate containing sample barcode/Illumina sequencing primers. 2x PCR mix from the kit was added, and PCR was performed according to the manufacturer's instructions. After PCR, samples were pooled, purified using a MinElute PCR Purification Kit (Qiagen, cat# 28,004) and diluted for sequencing on the Illumina MiSeq platform generating 2 × 300 paired reads.

Sequencing reads were processed by removing the sequences with low quality (average qual <35) and ambiguous codons (N's) using the in-house pipeline. Paired amplicon reads are assembled using Flash 2.0. Chimeric amplicons were removed using UChime software (RRID: SCR_008057) (Robert C Edgar et al., 2011). Our automatic pipeline used the processed reads for operational taxonomic unit (OTU) generation based on a sequence similarity threshold of 97%. Each OTU was classified from phylum to genus level using the most updated Ribosomal Database Project (RDP) 2016 classifier and training set (RRID: SCR_006633). A taxonomic abundance table was generated with each row as bacterial taxonomic classification, each column as sample ID and each field with taxonomic abundance. The abundance of a given taxon in a sample was present as relative abundance (the read counts from a given taxon divided by total reads in the sample). We also used PICRUSt2 (RRID:SCR_022647) (Douglas et al., 2020) to predict the functional profiling of the bacterial communities by ancestral state reconstruction using 16S rRNA gene sequences. Following the protocol described by Valles-Colomer (Valles-Colomer et al., 2019), gut-brain module analysis was performed on the PICRUST2 results. Multiple testing correction of the Gut-Brain Modules was performed using the qvalue package (RRID:SCR_001073).

2.6. mWGS sequencing, data processing and metagenomics species detection

Libraries were constructed with an average insert size of 500 bases and then sequenced on the HiSeq 2,500 instrument producing 150 base read pairs from each fragment yielding ~3 million read pairs/sample. Following mWGS sequencing, sequence data was run through a quality control pipeline to remove poor-quality reads and sequencing artifacts. Sequencing adapters were first removed using TRIMMOMATIC (RRID: SCR_011848) (Bolger et al., 2014). Next, exact duplicates, low quality, low complexity reads and mouse DNA contamination were removed using GATK-Pathseq (RRID:SCR_005203) (Walker et al., 2018) pipeline with a k-mer based approach. For optimization of mouse DNA decontamination, we have built a new GATK-Pathseq 31-mer database by concatenating the following collection of DNA sequences: MM10_GRCm38 reference; sixteen diverse laboratory mouse reference genomes define strain-specific haplotypes and novel functional loci; NCBI UniVec clone vector sequences; repetitive element sequences from RepBase 23.02 database; and mouse gencode transcripts databases (v25). The final clean reads were used for taxonomic classification and metabolic function analysis for further downstream analysis.

An optimized GATK-Pathseq classification pipeline is time efficient and robust solution for taxonomic classification at the species level. This pipeline used BWA-MEM alignment (minimum 50 bp length at 95% identity). It mapped the final clean reads to the latest updated reference of microbial genomes built by concatenating RefSeq Release 99 (March 2nd, 2020) nucleotide FASTA sequence files of bacteria, viruses, archaea, fungi, and protozoa. Gatk-Pathseq all read counts of microbial species of all kingdoms are used for species abundance analysis.

2.7. Differential abundance analysis of microbial genes and metabolic pathways

The KEGG ortholog (KO) profiling was performed by HumanN2 (RRID:SCR_016280) (Franzosa et al., 2018). Using DESeq2 package (RRID:SCR_015687) (Love et al., 2014) dedicated to performing comparative metagenomics, the inference of abundance of genes and pathways was obtained and visualized using volcano plot. Because of the potential high false positive rate of DESeq (Weiss et al., 2017), we plotted raw and relative abundance to inspect the results. Following the protocol described by Valles-Colomer (Valles-Colomer et al., 2019), gut-brain module analysis was performed on the mWGS results. Multiple testing correction of the Gut-Brain Modules was performed using the qvalue package (RRID:SCR_001073).

2.8. Statistical analysis

High-throughput behavioral phenotyping data is known to be affected by unwanted sources of variation such as the date of testing, seasonal effects, and the effect of the tester. Before using this behavioral phenotyping data, we assessed and corrected for these. First, we performed an outlier analysis removing any phenotypes greater than 3 SD of the mean. Then we tested to determine if the tester or date of the test had significant effects, $p < 0.05$. If those variables were significant, they were added to a model, the residuals of which were then tested for normality. If those residuals were normally distributed, they would be used for downstream analysis. If the residuals were not normally distributed, they were

rank Z transformed. This process was performed on a large dataset of over 3,000 DO mice. A subset of which were used in IVSA and a subset of those for microbiome analysis as reported in this manuscript.

Microbial community analysis was performed by R version 3.5.1 (RRID:SCR_001905). Principal coordinate analysis (PCoA) plots, boxplots and heatmaps were generated for graphical visualization using Phyloseq, ggplot2 (RRID:SCR_014601) (Wickham, 2016) and ComplexHeatmap (RRID:SCR_017270) (Gu et al., 2016) packages. Richness was calculated as the number of OTUs present in each sample. The Shannon Diversity Index combined species richness, and the evenness was computed as $\Sigma p_i * \ln(p_i)$, where pi presents the proportional abundance of species. The non-parametric Wilcoxon or Kruskal-Wallis rank sum-tests were used for differential diversity or abundance between two or more groups and corrected for multiple comparisons by the Benjamini-Hochberg procedure. Beta diversity was analyzed at the OTU level using the Bray-Curtis distance for community abundance and the Jaccard distance for community presence/absence.

The among-group differences were determined using the permutational multivariate analysis of variance by the distance matrices (ADONIS). These tests compare the intragroup distances to the intergroup distances in a permutation scheme and then calculate a p-value. These functions are implemented in the Vegan package (RRID: SCR_011950) (Jari Oksanen et al., 2020). For all permutation tests, we used 10,000 permutations.

Association between taxa and behavioral variables was assessed by fitting the Generalized Linear Model-GLM (glm R function). This approach raises additionally interesting associations between bacteria and behavior related to Age and Sex. The residuals were not checked for normality, rather the GLM regression coefficients were standardized using lm. beta R function. The Benjamini-Hochberg procedure (FDR) was used to correct for multiple testing of taxa and behavioral test associations, with significance defined as FDR <0.1.

We also used multi-task learning for feature selection by fitting a GLM via penalized maximum likelihood model (LASSO-Least Absolute Shrinkage and Selection Operator) (glmnet R package RRID: SCR_015505) (Jerome Friedman et al., 2021). The GLM allows us to predict the association of a single microbe with a novelty test regarding sex and age covariates. The p-value will be adjusted for multiple testing. By contrast, LASSO assesses the influences of all dependent variables on all response variables, and no assumption was made. We pooled all 42 known genera as dependent variables against 35 novelty behaviors as response variables. Using LASSO, the estimates of the regression algorithm are shrunk toward zero by adding a penalized term in the loss function. Relevant genera with nonzero coefficients were selected as informative variables associated with all behavior variables from the model. Thus, LASSO model represent an alternative approach of GLM to identify bacteria that associated with novelty behavior results.

Data transformation or distance matrices greatly influences analytical outcomes of the microbiome data (Paul J McMurdie, 2014) Our study applied common microbiome data process protocols such as rarefication to remove bias from sequencing depth, and include both Bray-Curtis and Jaccard dissimilarity matrices to compute microbiome differences

between groups. However, different data handling approaches may lead to other associations structure and clustering results. Our results relayed largely on logarithms and a high proportion of zeros in the dataset. As a result, prediction and feature selection methods considerably depend on handling zeros.

2.9. Network analysis

Network analysis was performed using SParse InversE Covariance Estimation for Ecological Association Inference (SPIEC-EASI) (RRID: SCR_022646), which combines data transformation developed for compositional data and a graphical model inference framework assuming the underlying ecological association network (Zachary D. Kurtz et al., 2015). The network was built on filtered ACQ and FACQ microbial data (filtered 50% OTU prevalence) of DO mice. All novelty behaviors were integrated as equal to each OTU.

3. Results

3.1. Differences in novelty-related behavior between mice that acquire self-administration of cocaine and those that failed-to-acquire self-administration of cocaine

Each of the novelty-behavior phenotyping paradigms results in numerous measurements. Therefore, we selected the least redundant, yet still highly correlated measures of novelty; 24 open-field measures, six light-dark box measures, three hold board measures, and one novelty place preference measure to be correlated with the ability to acquire IVSA in a cohort of diversity outbred mice (n = 228). For the IVSA assay, mice were categorized as having acquired cocaine self-administration (acquired (ACQ) n = 128) if they reached the established criteria and were able to proceed to a dose-response curve, extinction, and reinstatement. Otherwise, they were categorized as failed-to-acquire (failed-to-acquire (FACQ) n = 100), in which case they never achieved the criterion of having acquired cocaine self-administration. If there was no effect of sex, data from both sexes were pooled.

12 of the 24 open field measures were significantly different ($p < 0.05$) between the ACQ and FACQ mice. The open field assay can be used as a measure of activity, exploration, and anxiety. Mice that travel more are more active, mice that spend more time in the perimeter than the center are more anxious and mice that move around a lot in the arena and the center are more exploratory (Crawley, 1985; Sukoff Rizzo and Crawley, 2017). ACQ mice traveled a greater total distance ($W = 7882$, $Z = -2.99$ $p = 0.002$, $r = 0.19$), spent a greater amount of time in the perimeter ($W = 7695$, $Z = -2.61$, $p = 0.008$, $r = 0.17$), center ($W = 7863$, $Z = -2.95$, $p = 0.003$, $r = 0.19$) and corners ($W = 7868$, $Z = -2.96$, $p = 0.002$, $r = 0.19$) and less time resting in the corner ($W = 5104$, $Z = -2.62$, $p = 0.008$, $r = 0.17$) or resting anywhere ($W = 4833$, $Z = -3.17$, $p = 0.001$, $r = 0.2$). However, as percent, the ACQ group did display an increased resting time in the center ($W = 7403$, $Z = -2.02$, $p = 0.04$, $r = 0.13$). Similar to time spent in each region, the ACQ mice traveled further in each region corner ($W = 7681$, $Z = -2.59$, $p = 0.009$, $r = 0.17$) perimeter ($W = 7634$, $Z = -2.49$, $p = 0.01$, $r = 0.16$) and center ($W = 7808$, $Z = -2.84$, $p = 0.004$, $r = 0.18$). Consistent with their total activity, ACQ mice also traveled a greater distance in the last 5 min ($W = 7563$, $Z = -2.35$, $p = 0.018$, $r = 0.15$) and has a greater total ambulatory time on average ($W = 7945$, $Z = -3.12$, $p = 0.001$ and $r = 0.20$). Of these twelve measures only six passed a stringent FDR rate of 0.05. Those

included total distance traveled, total time in corner, total time in center, total resting time, total distance traveled in center and total ambulatory time (Fig. 1A, Supp Table 2).

For the light-dark assay, two measures, the percent resting time in the light ($W = 7711$, $Z = -2.65$, $p = 0.008$, $r = 0.17$) and the percent time in the light ($W = 7670$, $Z = -2.57$, $p = 0.01$, $r = 0.17$), were significantly different between ACQ and FACQ mice Increased time in the light side suggests the mice are less fearful (Sukoff Rizzo and Crawley, 2017), although neither measure passed a stringent FDR of 0.05 (Fig. 1B, Supp Table 2). A high number of hole pokes are observed in mice given anxiolytics (Crawley, 1985) Of the three holeboard measures, only the total number of entries was significantly different between ACQ and FACQ mice ($W = 7385.5$, $Z = -1.99$, $p < 0.05$, $r = 0.13$), with ACQ mice having a greater number of hole pokes than FACQ mice (Fig. 1C, Supp Table 2). The measure of novelty place preference, proportion of movement on the novel side, was significantly different ($W = 5335$, $Z = -2.15$, $p = 0.03$, $r = 0.14$) between groups (Fig. 1C, Supp Table 2). Neither the holeboard nor the novelty place preference measures passed a stringent FDR of 0.05.

3.2. Sex differences in novelty behavior between ACQ mice and FACQ

Mice of both sexes were tested. If there was no effect of sex, the data from the mice were pooled. Sex significantly influenced some measured behaviors when we compared ACQ and FACQ (Fig. 1D, Supp Table 2). For open field assays, female ACQ mice moved significantly more in the in the center than female FACQ mice ($W = 1055$, $Z = -2.18$, $p = 0.03$, $r = 0.21$). Female ACQ mice moved a lesser distance in the perimeter ($W = 1727$, $Z = -2.04$, $p = 0.04$, $r = 0.19$), and spent less time in the perimeter ($W = 1049$, $Z = -2.22$, $p = 0.03$, $r = 0.21$). We did not observe any male specific associations.

3.3. Microbial composition of DO mice

The sampling depth average over 228 fecal samples was approximately 57,000 reads per sample. Using a cutoff of 25% of prevalence, we identified 347 OTUs. The rarefaction curve was highly consistent in terms of read depth related to species richness (data not shown). Firmicutes and Bacteroides were two major phyla of fecal pellets from the DO mice, with 58% and 34% relative abundance, respectively. *Firmicutes* to *Bacteroides* ratio was −4.9 (0.1–61.8) (Supp Fig. 1.) *Actinobacteria* is the third the most abundant phylum with about 7% of relative abundance. Six dominant genera presented 71% of microbial composition in the colon, such as *unclassified_Lachnospiraceae* (16.8%), *unclassified_Porphyromonadaceae* (15.6%), *Lactobacillus* (13%), unclassified_*Bacteroidales* (12.1%), *Eisenbergiella* (8%) and *Barnesiella* (6.5%). The cohort had an alpha diversity of 236 (111–320) for richness.

3.4. Microbial composition of the ACQ vs. FACQ groups of DO mice

There were no significant differences in the richness and Shannon diversity between two IVSA groups when separated by sex or combined. Jaccard distance for community presence/absence showed no difference between groups (data not shown). The microbial composition and abundance of DO mice stratified by sex and groups are illustrated in Fig. 2A. In general, the bacterial community was highly dissimilar and reflected strong inter-individual variability, which is expected in an outbred mouse population. PC1 accounted for 19.2%

of the variance and PC2 13.7% of the variance of total microbiome community (Fig. 2B). PERMANOVA analysis showed overall microbiome community structure at the OTU was significantly different between two IVSA groups (p = 0.035). Variance analysis revealed that IVSA groups accounted for only 0.8% (p = 0.035) of microbiome variation, smaller than the effects sex (R2 = 1.1%, p = 0.0018) and age (R2 = 2.2%, p = 9.999e-05). Thus, overall community structure is significantly different between ACQ and FACQ, but not as influential as the effects of age and sex. We then looked at the phylum level, where the mean relative abundance of *Firmicutes* that contain many butyrate-producing bacteria was lower in the ACQ group (56%) than in the FACQ group (60.8%). The relative abundance of Bacteroidetes was inversely higher in the ACQ group (36.4%) than in the FACQ group (30.9%), however these differences were not statistically significant between ACQ and FACQ across both sexes (Supp Fig. 2, Supp Table 3).

At the genus level, four bacterial genera were significantly different between the two groups including the dominant taxon *Barnesiella* (W = 7437, Z = −2.09, p = 0.035, r = 0.138) and three rarer genera *Ruminococcus* (W = 7801, Z = −2.15, p = 0.004, r = 0.19), *Robinsoniella* (W = 7458, Z = −2.15, p = 0.03, r = 0.14), and *Clostridium* IV (W = 5321, Z = −2.18, p = 0.03, r = 0.14) (Fig. 3A–D). The abundance of *Blautia* was lower in female ACQ mice (W = 1086.5, Z = −2.02, p = 0.04, r = 0.19), whereas *Lactobacillus* (W = 1319, Z = −2.55, p = 0.01, r = 0.17) differed only in males, where ACQ males had lower abundance than FACQ males (Fig. 3E and F). One quantitative metric that all mice tested on IVSA had in common was the number of doses administered under the 1.0 mg/kg acquisition dose. Any mouse that failed to acquire would have less than ten doses administered. The doses administered across all mice and relative abundances of *Robinsoniella* (R = 0.15) and *Clostridium IV* (R = −0.13) were significantly correlated (p < 0.05) (Fig. 3G and H, Sup Fig. 3).

3.5. Association of the microbiome and behavior in ACQ group

To understand the relationships between the gut microbiome and novelty behaviors of DO mice, we performed GLM with age and sex covariates. Because the microbiome was significantly different between ACQ and FACQ groups, GLM was performed in ACQ and FACQ groups separately. In ACQ group, 57 significant associations were observed ($p < 0.05$), but none was significant after p value corrections for multiple testing (Fig. 4A, Supp Table 4). However, *Barnesiella* had the highest regression coefficient with the novelty preference place test (0.28, p = 0.001), such that increased *Barnsiella* was associated with increased preference for novel side or novelty. *Robinsoniella* had the largest number of associations with ten open field tests, such that increased activity and decreased anxiety were associated with increased *Robinsoniella* abundance. *Blautia* and *Parvibacter* had five significant associations with behavior in the open field tests, while *Lactobacillus* and *Marvinbryantia* had four significant associations with open field assay. Because no associations passed FDR correction, we sought to validate those findings using LASSO analysis. When carrying out the Lasso regression analysis with all genera, ten genera were found to be associated with thirty-five novelty behaviors and these genera were all *Clostridia* class (*Firmicutes* phylum) (Fig. 4B, Supp Table 5). The seven most influential bacterial general were *Blautia, Christensenella, Murimonas, Flavonifractor, Robinsoniella, and Anaerofustis*, with the biggest effects on the behaviors in ACQ mice (L2 sum

coefficients of 182.9, 138.7, 51.7, 44.3, 36.5, and 20, respectively), with *Coprococcus* (19.8) just behind.

3.6. Association of microbiome and behavior in the FACQ group across methods

There were 71 significant associations ($p < 0.05$) between the gut microbiome and behaviors in FACQ group, which is larger than the number of associations in the ACQ group (57), although none passed a stringent FDR. (Fig. 4A). *Lactobacillus* and *Anaerostipes* had the largest number of significant positive and negative associations, respectively. An increase in *Lactobacillus* was associated with decreased values in the light-dark and open field, suggesting that FACQ mice are less active and more anxious in the presence of *Lactobacillus*. *Butyricicoccus, Enterococcus, Escherichia/Shigella, Lachnospiracea_incertae_sedis* and *Robinsoniella generated* significant correlations with the novelty-related behavior tests. Interestingly, different from other microbes, *Butyricicoccus* and *Escherichia/Shigella* were the only two that predominantly correlated to behaviors in the light-dark assay. However, *Butyricicoccus* was positively associated with the light-dark tests, while *Escherichia/Shigella* was negatively correlated to these behaviors. LASSO analysis revealed that the top ten genera that were most important predicted by Lasso regression were all *Clostridia* class (Fig. 4B). Interestingly, the coefficient of regression was importantly lower in FACQ than in ACQ mice. For example, *Christensenella* was the most influential microbe, with a coefficient of 116.5 in FACQ mice compared to 138.8 in ACQ mice.

3.7. Common and unique associations between the microbiome and behaviors in ACQ and FACQ groups

A common bacterium that repeatedly had significant associations with novelty behaviors in both groups with different statistical methods is the *Robinsoniella* genus. Common associations in both groups reflect similar predicted microbial gene functions, including those involved in metabolic pathways. LASSO analysis also revealed several common short-chain fatty acid-producing bacteria associated with novelty behaviors in both groups. Among those microbes already identified as associated with novelty behaviors through GLM *Clostridium XlVb*, *Clostridium IV,* and *Intestinimonas* were also associated through LASSO. In GLM, there are several identical associations between a second *Ruminococcus* species (*Ruminococcus 2)*, *Clostridium IV* and novelty preference place, *Robinsoniella* and three open field tests (total distance traveled in the center, total resting time, and total time in the center) across groups. *Marvinbryantia* was positively associated with total distance traveled in the corner in ACQ mice and negatively associated in FACQ.

Among 42 analyzed genera, 15 uniquely correlated to novelty behaviors in ACQ mice were mostly from *Clostridia* class such as *Coprococcus*, *Anaerovorax*, *Lactonifactor, Ruminococcus, Oscillibacter, Clostridium IV, Syntrophococcus, and Intestinimonas*. Others were from different classes, such as *Barnesiella* and Alistipes (*Bacteroidia* class), *Erysipelotrichaceae_incertae_sedis,* and *Coprobacillus* (*Erysipelotrichia* class), *Akkermansia* (*Verrucomicrobiae* class) *and Parvibacter* (*Actinobacteria* class). LASSO analysis identified *Coprococcus* as an influential microbe of novelty-related behaviors in ACQ mice. Its abundance was negatively correlated to most behaviors in the open field and the light-dark assays. In FACQ mice, we found only three microbial

groups uniquely correlated to behaviors, two of which belonged to the *Clostridia* class (*Anaerotruncus*, *Lachnospiracea_incertae_sedis*) and one from the *Gammaproteobacteria* class (*Escherichia.Shigella*). A complete compassion across the GLM and LASSO analysis can be found in Supp Table 6.

3.8. Network analysis of the microbiome, novelty behaviors, and cocaine IVSA

Network analysis correlating bacterial abundance, novelty behaviors, and the number of infusions of cocaine self-administered revealed important associations between *Coprococcus* and *Actinobacteria* in FACQ mice. The network prototype was built on filtered microbial data (>50% of OTU prevalence), and all novelty behaviors were integrated, with each novelty behavior being considered a node (Fig. 5A). Consistently present OTUs were similar between ACQ mice and FACQ mice. The network presented 241 nodes and 342 edges for ACQ mice, while the FACQ mice network had 243 nodes and 346 edges. The interactions in both networks were more likely dominated between OTUs of the highest dominant phylum *Firmicutes* (195 connections in ACQ mice, 199 connections in FACQ mice) and between OTUs of Bacteroidetes (43 connections in ACQ mice, 47 connections in FACQ mice). Moreover, the interactions between OTUs of *Firmicutes-Bacteroidetes* and between OTUs of *Firmicutes-Actinobacteria* were higher in FACQ mice (21 and 21 respectively) than in ACQ mice (17 and 13 respectively). Among the interactions between microbial taxa and novelty behaviors, it is interesting to note that *Coprococcus* (OTU_116) (also identified in the LASSO analysis) and *Lactobacillus* (OTU_1) were the two common bacteria correlated to several novelty tests with an almost inverse relationship. However, in ACQ mice, *Coprococcus* OTU was negatively associated with percent resting time in the light (LD3), percent resting time in the perimeter (OFA21) and *Clostridium IV* (OTU_193). In FACQ mice, *Coprococcus* (OTU_116) was negatively correlated to novelty place preference (NPP1), percent distance in the center (OFA13) and percent resting time in the corner (OFA20) of open field assay (Fig. 5B). We also observed associations between *Lactobacillus* (OTU_1) and behaviors in open field assay in both groups; there was a positive association with percent distance in the perimeter (OFA15) for FACQ mice, and with percent resting time in the perimeter (OFA21) for ACQ mice. 1.0 mg/kg cocaine infusion (IVSA) was associated with percent resting time in the center (OFA19) in FACQ, and with percent time in the corner (OFA17) and percent resting time in the corner (OFA20) in ACQ mice. An important difference between the two networks was the negative association between *Coprococcus* (OTU_116) and *Enterohardus* (OTU_58, *Actinobacteria* phylum) in FACQ mice, an important node in the network that generated ten connections with mostly all other species of *Actinobacteria* phylum (*Enterohardus* (OTU_7, OTU_76), *Parvibacter* (OTU_229), and *unclassified_Coriobacteriaceae* (OTU_24, OTU_249, OTU_208, OTU_33). This association was absent in ACQ mice.

3.9. Functional profiling and mWGS analysis show various aspects of glutamate metabolism

Using PICRUSt2 on the 16S data, we identified 32 gut-brain modules as significantly ($p < 0.05$) different between the microbiome of ACQ and FACQ mice and two with qvalue <0.05 (Fig. 6A and B, Table 1). Five modules mapped to the GABA I synthesis KO, 18 to glutamate, and seven to propionate degradation/synthesis, in addition to one to dopamine

and gamma-hydroxybutyric acid degradation KO (GHB). From mWGS data on a subset of 96 mice, we identified eight gut-brain modules that differed significantly ($p < 0.05$) between ACQ and FACQ group (Fig. 6C and D, Table 2). Half of those modules were related to glutamate, while the others were methionine biosynthesis, acetate synthesis I, isovaleric acid synthesis I and *S*-adenosylmethionine synthesis. Both methodologies identified other-glutamate modules KO1919 and KO10004 as significantly up-regulated in mWGS and 16S. These glutamate KO were glutamine-cysteine ligase and glutamate/aspartate transport system ATP binding protein respectively. Pathway analysis of the mWGS data showed three pathways upregulated greater than 0.5 fold, glutamate degradation PWY-4321, peptidoglycan biosynthesis IV PWY-6471, and heme biosynthesis II HEMESYN2. PWY. One pathway, fatty acid salvage PWY-7094, was downregulated at least 0.5 fold in FACQ mice. (Fig. 6E–G, Table 3). The source of the PWY-4321 gene produced from the mWGS sequencing data indicated that the *Lactobacillius reuteri* was one of the sources of these pathway members (Supp Table 7). We looked at the three most abundant species of *Lactobacillus (L.reuteri, L. gasseri, L. intestinalis*) and found that they were significantly ($p < 0.05$) increased in FACQ mice compared to ACQ mice (Fig. 6H). These species are well known for their immunomodulatory effects on the central nervous system and anxiety-like behavior. Furthermore, *Lactobacillus* species are known to produce GABA and glutamate (Ahmad et al., 2001). Together functional profiling of 16S and mWGS data showed enriched trends toward glutamate biosynthesis in the FACQ group with the results showing remarkable agreement between the two sequencing types.

4. Discussion

Understanding the complex relationship between novelty-related behaviors, intravenous self-administration of drugs, and gut microbiome will uncover new insights into gut-brain communication and addiction and addiction-like behaviors. Our study presents a large microbiome dataset from the feces, novelty-related behavior assays and intravenous self-administration to assess the bi-directional gut-brain axis communication in a random population of DO mice. Unlike inbred mice, DO mice have endogenously varied microbiomes under otherwise highly similar environmental conditions. This enables us to make connections between the differences in the abundance or presence of microbial groups with differences in novelty-related behaviors. Performing these studies in replicates of an inbred strain of mice would not show the degree to variation in abundance we observe without manipulation, such as diet changes, antibiotic ablation, or probiotic treatment. Using the DO mice population, we identified that abundance of three genera, *Barnesiella, Ruminococcus, and Robinsoniella,* positively correlated with drug self-administration behavior acquisition and one genera, *Clostridium* IV, was negatively correlated with acquisition behavior. We used these differences to nominate metabolic pathways that may influence gut-brain communication under these conditions and identified those involved in glutamate pathways. The inability to control for environmental conditions that strongly influence changes in the gut microbiome in humans makes correlative associations between the microbiome and behavior very challenging.

Male and female mice harbor distinct gut microbiome (McGee and Huttenhower, 2021) that likely influence biological differences. Fecal transplantation of the microbiome derived

from male mice altered sex hormone levels in female recipients (Markle et al., 2013). An addiction-relevant study utilizing a heterogenous population of rats (Peterson et al., 2020) —similar to the mouse population described here—showed a sex-dependent association between microbiome composition and addiction-related behaviors of 'sign-tracking' and 'goal-tracking'. They found, for example, several measures of impulsivity correlated with the abundance of *Barnsiella* only in female rats. Our study also uncovered sex-specific effects, including decreased *Lactobacillus* abundance in male FACQ mice. We also measured sex-specific effects in novelty-related behaviors, which have been correlated with a propensity toward addiction. The amount of time ACQ females spend in the center of an open field is higher; similarly, the amount of time they spent at the perimeter is lower. Female ACQ mice also moved a smaller distance on the perimeter than the FACQ females.

In previous studies, the abundance of *Barnesiella*, an SCFA-producing microbe, was increased tenfold in colonic contents in response to cocaine (Chivero et al., 2019). In the same survey, *Pseudoflavonifractor* was decreased by cocaine administration. In this study, *Barnesiella* correlated with novelty preference and percent center time in the ACQ group using the GLM approach. *Pseudoflavonifractor* was associated with the number of light-dark transitions in the ACQ group and two open field measures in the FACQ group. In outbred rats, cecal *Barnesiella* abundance was negatively correlated with locomotor activity in a sex-specific fashion (Peterson et al., 2020). *Fusicatenibacter* in both groups was associated with novelty preference and, in a human study, was one of the taxa related to individuals undergoing a depressive episode (Jiang H-Y, 2020). Here we associate the microbial abundance of four genera with the propensity of mice to acquire self-administration of cocaine. Others have shown that within one inbred strain, a subset of mice often fails to acquire self-administration (Roberts et al., 2018). Roberts et al. looked at eight different inbred strains and found an acquisition rate anywhere from 100% (I/LnJ) to 47% (FVN/NJ). Due to cage effects, parent of origin effects, or other environmental variables, these mice may have microbiome differences that influence their ability to acquire IVSA. Diet can have a profound impact on behavior, as was recently illustrated by the Linsenbardt group; they showed that the development of alcohol front-loading was abolished by switching C57BL/6 J mice from a LabDiet 5001 to a Teklad 2920x rodent diet (Maphis et al., 2022). The role of the microbiome was not addressed in that work. Diet and environment are the biggest drivers of microbiome composition in a genetically inbred population (Bubier et al., 2021). Work using the same assays of binge drinking in C57BL/6 J mice with a 2-week antibiotic pretreatment significantly increased alcohol consumption (Reyes et al., 2020). This increased consumption could be reversed by sodium butyrate supplementation (Reyes et al., 2022).

SUD is commonly associated with several comorbid psychiatric traits, such as anxiety and depression (Abuse, 2020). These traits are often modeled in animals using measurable behaviors, such as impulsivity, novelty-seeking, and risk-taking (Baj et al., 2019). We measured addiction predictive behaviors in DO mice and found that ACQ mice are more active and exploratory (e.g., distance traveled in the open field) and less anxious (e.g., total time in the center) than FACQ mice in the open field. These connections were supported by measurements in light-dark assays, in which the percent resting time in the light and percent time in the light were higher in ACQ compared to FACQ mice. This suggests

that mice that go on to ACQ have less fear of the light side than those that FACQ. ACQ mice also demonstrated more curiosity and were more exploratory in the hole board assay when compared to FACQ mice. The only assay that failed to reflect known risk factors associated with SUD was the novelty place preference assay. Here, mice that FACQ were more active in the novel side, therefore, more novelty-seeking than the ACQ mice. One possible explanation is that the order of the assays influenced the results. The novelty place preference assay was conducted on the fourth day of testing, and the mice may have become acclimated to being tested. Our studies also found that anxiety-like behaviors were not predictive of whether mice would go on to acquire cocaine self-administration, but exploratory, risk-taking behaviors were.

The role of the microbiome in behavior has been well established. Germ-free (GF) mice exhibit abnormal immune- and neuro-development and display abnormal behaviors such as increased locomotor activity in the open field (Neufeld et al., 2011). The behavioral abnormalities, reflecting decreased anxiety, extend to time spent in the center of the open fields and increased time spent on the light side of the light-dark apparatus (Diaz Heijtz et al., 2011). The changes observed in the GF mice, specifically the open field center time and center distance, were shown to not be reversible by colonization with microbiota from a specific pathogen-free facility (Chen et al., 2017). However, probiotic treatment of GF mice with live *Lactobacillus plantarum* PS128 resulted in increased total distance traveled and decreased center time in the open field. Recent findings have even shown that a gut-derived metabolite such as 4-ethylphenyl sulfate influences anxiety-like behaviors in mice through the alteration of oligodendrocyte function and myelin pattering in the brain (Needham et al., 2022). Transplant studies into mice from people with schizophrenia vs. controls resulted in increased distance traveled in the open field and increased center time. This behavior change suggested that the dysbiosis seen in schizophrenia can function by modulating the hippocampus's glutamate-glutamine-GABA cycle (Zheng et al., 2019). The association of *Lactobacillus* and glutamate metabolism with cocaine IVSA acquisition is very interesting. Imaging studies have shown that BALBc/J mice given *Lactobacillus rhamnosus,* although not one of the species identified here, resulted in increases in brain GABA, *N*-acetyl aspartate and glutamate (Janik et al., 2016).

Our analysis of the metabolic pathways encoded by the microbiome as measured by both 16S and mWGS supports a key differential role in glutamate metabolism, potentially encoded by the three species of *Lactobacillus* identified here. Glutamate plays an obvious role in the biosynthesis of proteins, but it is also important for synaptic transmission and plasticity. Glutamate in the central and enteric nervous system is also a major excitatory neurotransmitter (Filpa et al., 2016) and is the precursor of the inhibitory neurotransmitter GABA. Dysregulation of GABA the brain is associated with various nervous system disorders (Meldrum, 2000). Our findings demonstrate an increase in glutamate degradation IV in mice that ACQ, consistent with the role of glutamate in addiction-like behaviors (Kalivas, 2004, 2009; Koob and Nestler, 1997; Koob and Volkow, 2016). Others studies, comparing conventional and GF mice, have shown that an intact gut microbiome directly influences brain glutamate (Kawase et al., 2017). Importantly, there are glutamate receptors on the epithelial cells of the gut, splanchnic, vagal and pelvic afferents (Chun et al., 2009; Filpa et al., 2016; Furness et al., 2014), further supporting the role of glutamate in regulating

the gut-brain axis. Work in rats has shown that early stress, through maternal separation, reduces the rewarding properties of cocaine and that altering glutamatergic signaling in adolescent rats restores the cocaine reward effect (O'Connor et al., 2015). The work presented here that measures increased glutamate degradation in mice that go on to ACQ IVSA, together with that of O'Conner, suggests that reducing glutamatergic signaling may be a viable strategy for treating individuals with SUD.

The pathway data from PICRUSt analysis of 16S data and from mapping mWGS provide only a snapshot of metabolic potential at the moment the fecal sample was collected. Although quite distinct at the bacterial species level, 80% of known function of the microbiome is shared between mice and humans (Beresford-Jones et al., 2022). Thus, we believe that pathways encoded by the microbiome may be more informative than the specific microbes themselves when translating findings from mice to human. The glutamate degradation pathways observed in mice, possibly attributed to three *Lactobacillus* species, may be found in the human microbiome encoded by other genera of microbes. While not addressed here, future genome-wide association studies of this mouse population will enable us to identify the genetic loci associated with the presence or abundance of certain microbes.

This study demonstrates, by using multiple approaches in an outbred mouse population with genetic variation similar to the human population, that certain bacteria are specifically associated with novelty response and its predisposing effects on intravenous self-administration of cocaine. The strongest associations were the relative abundance of *Barnesiella, Ruminococcus, Robinsoniella* and *Clostridium* IV with the ability to self-administer cocaine. In addition, the sex-specific association of *Lactobacillus* with IVSA supports a role for microbial glutamate metabolism in the ability to self-administer cocaine. This finding provides evidence of alternate pathways that can be modulated to alter addiction behavior through manipulating the microbiome using metabolites or pre-and probiotics.

Supplementary Material

Refer to Web version on PubMed Central for supplementary material.

Acknowledgments

NIH R01 DA037927 to EJC; NIH P50 DA039841 to EJC; NIH U01 DA043809 to JAB/GW. Cocaine hydrochloride was provided by NIDA Drug Supply Program. We thank Sara Cassidy for close reading and editing of this manuscript. Graphical abstract created with BioRender.com.

Data availability

Mouse phenotype data @ CSNA03 https://phenome.jax.org. 16S data are upload to SRA SUB12113840

Abbreviations

DO	diversity outbred

IVSA	intravenous self-administration
OTU	operational taxonomic unit
PICRUSt	Phylogenetic Investigation of Communities by Reconstruction of Unobserved States
SCFA	short chain fatty acids
WGS	whole genome sequencing
ACQ	Acquired cocaine self-administration phenotype
FACQ	Failed to acquire cocaine self-administration behavior
KO	KEGG Orthology
GBM	gut-brain modules
BBB	Blood Brain Barrier

References

Abuse N.I.o.D., 2020. Common Comorbidities with Substance Use Disorders Research Report (Bethesda, MD).

Ahmad B, Mufti KA, Farooq S, 2001. Psychiatric comorbidity in substance abuse (opioids). J. Pakistan Med. Assoc. 51, 183–186.

Alamoudi MU, Hosie S, Shindler AE, Wood JL, Franks AE, Hill-Yardin EL, 2022. Comparing the gut microbiome in autism and preclinical models: a systematic review. Front. Cell. Infect. Microbiol. 12, 905841. [PubMed: 35846755]

American Psychiatric Association., American Psychiatric Association, DSM-5 Task Force, 2013. Diagnostic and Statistical Manual of Mental Disorders : DSM-5. American Psychiatric Association, Washington, D.C.

Baj A, Moro E, Bistoletti M, Orlandi V, Crema F, Giaroni C, 2019. Glutamatergic signaling along the microbiota-gut-brain Axis. Int. J. Mol. Sci. 20.

Belin D, Deroche-Gamonet V, 2012. Responses to novelty and vulnerability to cocaine addiction: contribution of a multi-symptomatic animal model. Cold Spring Harb Perspect Med 2.

Beresford-Jones BS, Forster SC, Stares MD, Notley G, Viciani E, Browne HP, Boehmler DJ, Soderholm AT, Kumar N, Vervier K, Cross JR, Almeida A, Lawley TD, Pedicord VA, 2022. The Mouse Gastrointestinal Bacteria Catalogue enables translation between the mouse and human gut microbiotas via functional mapping. Cell Host Microbe 30, 124–138 e128. [PubMed: 34971560]

Bolger AM, Lohse M, Usadel B, 2014. Trimmomatic: a flexible trimmer for Illumina sequence data. Bioinformatics 30, 2114–2120. [PubMed: 24695404]

Bubier JA, Philip VM, Quince C, Campbell J, Zhou Y, Vishnivetskaya T, Duvvuru S, Blair RH, Ndukum J, Donohue KD, Foster CM, Mellert DJ, Weinstock G, Culiat CT, O'Hara BF, Palumbo AV, Podar M, Chesler EJ, 2020. A microbe associated with sleep revealed by a novel systems genetic analysis of the microbiome in collaborative cross mice. Genetics 214, 719–733. [PubMed: 31896565]

Bubier JA, Chesler EJ, Weinstock GM, 2021. Host genetic control of gut microbiome composition. Mamm. Genome 32, 263–281. [PubMed: 34159422]

Buffington SA, Dooling SW, Sgritta M, Noecker C, Murillo OD, Felice DF, Turnbaugh PJ, Costa-Mattioli M, 2021. Dissecting the contribution of host genetics and the microbiome in complex behaviors. Cell 184, 1740–1756 e1716. [PubMed: 33705688]

Cervantes MC, Laughlin RE, Jentsch JD, 2013. Cocaine self-administration behavior in inbred mouse lines segregating different capacities for inhibitory control. Psychopharmacology (Berl) 229, 515–525. [PubMed: 23681162]

Chen JJ, Zeng BH, Li WW, Zhou CJ, Fan SH, Cheng K, Zeng L, Zheng P, Fang L, Wei H, Xie P, 2017. Effects of gut microbiota on the microRNA and mRNA expression in the hippocampus of mice. Behav. Brain Res. 322, 34–41. [PubMed: 28093256]

Chen LL, Abbaspour A, Mkoma GF, Bulik CM, Ruck C, Djurfeldt D, 2021. Gut microbiota in psychiatric disorders: a systematic review. Psychosom. Med. 83, 679–692. [PubMed: 34117156]

Chesler EJ, Miller DR, Branstetter LR, Galloway LD, Jackson BL, Philip VM, Voy BH, Culiat CT, Threadgill DW, Williams RW, Churchill GA, Johnson DK, Manly KF, 2008. The collaborative cross at oak ridge national laboratory: developing a powerful resource for systems genetics. Mamm. Genome 19, 382–389. [PubMed: 18716833]

Chesler EJ, Gatti DM, Morgan AP, Strobel M, Trepanier L, Oberbeck D, McWeeney S, Hitzemann R, Ferris M, McMullan R, Clayshultle A, Bell TA, Manuel de Villena FP, Churchill GA, 2016. Diversity outbred mice at 21: maintaining allelic variation in the face of selection. G3 (Bethesda) 6, 3893–3902. [PubMed: 27694113]

Chivero ET, Ahmad R, Thangaraj A, Periyasamy P, Kumar B, Kroeger E, Feng D, Guo ML, Roy S, Dhawan P, Singh AB, Buch S, 2019. Cocaine induces inflammatory gut milieu by compromising the mucosal barrier integrity and altering the gut microbiota colonization. Sci. Rep. 9, 12187. [PubMed: 31434922]

Chun KS, Lao HC, Trempus CS, Okada M, Langenbach R, 2009. The prostaglandin receptor EP2 activates multiple signaling pathways and beta-arrestin 1 complex formation during mouse skin papilloma development. Carcinogenesis 30, 1620–1627. [PubMed: 19587094]

Churchill GA, Airey DC, Allayee H, Angel JM, Attie AD, Beatty J, Beavis WD, Belknap JK, Bennett B, Berrettini W, Bleich A, Bogue M, Broman KW, Buck KJ, Buckler E, Burmeister M, Chesler EJ, Cheverud JM, Clapcote S, Cook MN, Cox RD, Crabbe JC, Crusio WE, Darvasi A, Deschepper CF, Doerge RW, Farber CR, Forejt J, Gaile D, Garlow SJ, Geiger H, Gershenfeld H, Gordon T, Gu J, Gu W, de Haan G, Hayes NL, Heller C, Himmelbauer H, Hitzemann R, Hunter K, Hsu HC, Iraqi FA, Ivandic B, Jacob HJ, Jansen RC, Jepsen KJ, Johnson DK, Johnson TE, Kempermann G, Kendziorski C, Kotb M, Kooy RF, Llamas B, Lammert F, Lassalle JM, Lowenstein PR, Lu L, Lusis A, Manly KF, Marcucio R, Matthews D, Medrano JF, Miller DR, Mittleman G, Mock BA, Mogil JS, Montagutelli X, Morahan G, Morris DG, Mott R, Nadeau JH, Nagase H, Nowakowski RS, O'Hara BF, Osadchuk AV, Page GP, Paigen B, Paigen K, Palmer AA, Pan HJ, Peltonen-Palotie L, Peirce J, Pomp D, Pravenec M, Prows DR, Qi Z, Reeves RH, Roder J, Rosen GD, Schadt EE, Schalkwyk LC, Seltzer Z, Shimomura K, Shou S, Sillanpaa MJ, Siracusa LD, Snoeck HW, Spearow JL, Svenson K, Tarantino LM, Threadgill D, Toth LA, Valdar W, de Villena FP, Warden C, Whatley S, Williams RW, Wiltshire T, Yi N, Zhang D, Zhang M, Zou F, Complex Trait C, 2004. The Collaborative Cross, a community resource for the genetic analysis of complex traits. Nat. Genet. 36, 1133–1137. [PubMed: 15514660]

Ciosek J, Guzek JW, 1992. Thyrotropin-releasing hormone (TRH) and vasopressin and oxytocin release: in vitro as well as in vivo studies. Exp. Clin. Endocrinol. 100, 152–159. [PubMed: 1305067]

Ciosek J, Guzek JW, Orlowska-Majdak M, 1992. Neurohypophysial vasopressin and oxytocin as influenced by (6R)-5,6,7,8-tetrahydro-alpha-biopterin in euhydrated and dehydrated rats. Biol. Chem. Hoppe Seyler 373, 1079–1083. [PubMed: 1418678]

Cook RR, Fulcher JA, Tobin NH, Li F, Lee DJ, Woodward C, Javanbakht M, Brookmeyer R, Shoptaw S, Bolan R, Aldrovandi GM, Gorbach PM, 2019. Alterations to the gastrointestinal microbiome associated with methamphetamine use among young men who have sex with men. Sci. Rep. 9, 14840. [PubMed: 31619731]

Crawley JN, 1985. Exploratory behavior models of anxiety in mice. Neurosci. Biobehav. Rev. 9, 37–44. [PubMed: 2858080]

Cryan JF, Mazmanian SK, 2022. Microbiota-brain axis: context and causality. Science 376, 938–939. [PubMed: 35617385]

Day AW, Kumamoto CA, 2022. Gut microbiome dysbiosis in alcoholism: consequences for health and recovery. Front. Cell. Infect. Microbiol. 12, 840164. [PubMed: 35310839]

Diaz Heijtz R, Wang S, Anuar F, Qian Y, Bjorkholm B, Samuelsson A, Hibberd ML, Forssberg H, Pettersson S, 2011. Normal gut microbiota modulates brain development and behavior. Proc. Natl. Acad. Sci. U. S. A. 108, 3047–3052. [PubMed: 21282636]

Dickson PE, Ndukum J, Wilcox T, Clark J, Roy B, Zhang L, Li Y, Lin DT, Chesler EJ, 2015. Association of novelty-related behaviors and intravenous cocaine self-administration in Diversity Outbred mice. Psychopharmacology (Berl) 232, 1011–1024. [PubMed: 25238945]

Douglas GM, Maffei VJ, Zaneveld JR, Yurgel SN, Brown JR, Taylor CM, Huttenhower C, Langille MGI, 2020. PICRUSt2 for prediction of metagenome functions. Nat. Biotechnol. 38, 685–688. [PubMed: 32483366]

Filpa V, Moro E, Protasoni M, Crema F, Frigo G, Giaroni C, 2016. Role of glutamatergic neurotransmission in the enteric nervous system and brain-gut axis in health and disease. Neuropharmacology 111, 14–33. [PubMed: 27561972]

Flagel SB, Waselus M, Clinton SM, Watson SJ, Akil H, 2014. Antecedents and consequences of drug abuse in rats selectively bred for high and low response to novelty. Neuropharmacology 76 Pt B, 425–436. [PubMed: 23639434]

Franzosa EA, McIver LJ, Rahnavard G, Thompson LR, Schirmer M, Weingart G, Lipson KS, Knight R, Caporaso JG, Segata N, Huttenhower C, 2018. Species-level functional profiling of metagenomes and metatranscriptomes. Nat. Methods 15, 962–968. [PubMed: 30377376]

Furness JB, Callaghan BP, Rivera LR, Cho HJ, 2014. The enteric nervous system and gastrointestinal innervation: integrated local and central control. Adv. Exp. Med. Biol. 817, 39–71. [PubMed: 24997029]

Gu Z, Eils R, Schlesner M, 2016. Complex heatmaps reveal patterns and correlations in multidimensional genomic data. Bioinformatics 32, 2847–2849. [PubMed: 27207943]

Jalodia R, Abu YF, Oppenheimer MR, Herlihy B, Meng J, Chupikova I, Tao J, Ghosh N, Dutta RK, Kolli U, Yan Y, Valdes E, Sharma M, Sharma U, Moidunny S, Roy S, 2022. Opioid use, gut dysbiosis, inflammation, and the nervous system. J. Neuroimmune Pharmacol. 17, 76–93. [PubMed: 34993905]

Janik R, Thomason LAM, Stanisz AM, Forsythe P, Bienenstock J, Stanisz GJ, 2016. Magnetic resonance spectroscopy reveals oral Lactobacillus promotion of increases in brain GABA, N-acetyl aspartate and glutamate. Neuroimage 125, 988–995. [PubMed: 26577887]

Jari Oksanen FGB, Michael Friendly, Roeland Kindt, Pierre Legendre, Dan McGlinn, Minchin Peter R., O'Hara RB, , Gavin Simpson, Solymos L, Peter Henry, Stevens M, Eduard H, Szoecs Wagner, Helene, 2020. Vegan Package 298.

Jerome Friedman TH, Tibshirani Rob, Narasimhan Balasubramanian, Tay Kenneth, Simon Noah, Qian Junyang, 2021. Lasso and elastic-net regularized generalized linear models. Package "glmnet".

Jiang H-Y PLY, Zhang X, Zhang Z, Zhou Y-Y, Ruan B, 2020. Altered gut bacterial–fungal interkingdom networks in patients with current depressive episode. Brain Behav 10.

Kalivas PW, 2004. Glutamate systems in cocaine addiction. Curr. Opin. Pharmacol. 4, 23–29. [PubMed: 15018835]

Kalivas PW, 2009. The glutamate homeostasis hypothesis of addiction. Nat. Rev. Neurosci. 10, 561–572. [PubMed: 19571793]

Kawase T, Nagasawa M, Ikeda H, Yasuo S, Koga Y, Furuse M, 2017. Gut microbiota of mice putatively modifies amino acid metabolism in the host brain. Br. J. Nutr. 117, 775–783. [PubMed: 28393748]

Kiraly DD, Walker DM, Calipari ES, Labonte B, Issler O, Pena CJ, Ribeiro EA, Russo SJ, Nestler EJ, 2016. Alterations of the host microbiome affect behavioral responses to cocaine. Sci. Rep. 6, 35455. [PubMed: 27752130]

Kliethermes CL, Crabbe JC, 2006. Genetic independence of mouse measures of some aspects of novelty seeking. Proc. Natl. Acad. Sci. U. S. A. 103, 5018–5023. [PubMed: 16551746]

Koob GF, Nestler EJ, 1997. The neurobiology of drug addiction. J. Neuropsychiatry Clin. Neurosci. 9, 482–497. [PubMed: 9276849]

Koob GF, Volkow ND, 2016. Neurobiology of addiction: a neurocircuitry analysis. Lancet Psychiatr. 3, 760–773.

Kurtz Zachary, Miraldi D, Emily R, Littman Dan, Blaser R, Martin J, Bonneau Richard, A., 2015. Sparse and compositionally robust inferenceof microbial ecological networks. PLoS Comput. 11, e1004226.

Liu WH, Chuang HL, Huang YT, Wu CC, Chou GT, Wang S, Tsai YC, 2016. Alteration of behavior and monoamine levels attributable to Lactobacillus plantarum PS128 in germ-free mice. Behav. Brain Res. 298, 202–209. [PubMed: 26522841]

Love MI, Huber W, Anders S, 2014. Moderated estimation of fold change and dispersion for RNA-seq data with DESeq2. Genome Biol. 15, 550. [PubMed: 25516281]

Maphis NM, Huffman RT, Linsenbardt DN, 2022. The development, but not expression, of alcohol front-loading in C57BL/6J mice maintained on LabDiet 5001 is abolished by maintenance on Teklad 2920x rodent diet. Alcohol Clin. Exp. 46, 1321–30.

Markle JG, Frank DN, Mortin-Toth S, Robertson CE, Feazel LM, Rolle-Kampczyk U, von Bergen M, McCoy KD, Macpherson AJ, Danska JS, 2013. Sex differences in the gut microbiome drive hormone-dependent regulation of autoimmunity. Science 339, 1084–1088. [PubMed: 23328391]

McGee JS, Huttenhower C, 2021. Of mice and men and women: sexual dimorphism of the gut microbiome. Int J Womens Dermatol 7, 533–538. [PubMed: 35005176]

Meldrum BS, 2000. Glutamate as a neurotransmitter in the brain: review of physiology and pathology. J. Nutr. 130, 1007S–1015S. [PubMed: 10736372]

Mello NK, Negus SS, 1996. Preclinical evaluation of pharmacotherapies for treatment of cocaine and opioid abuse using drug self-administration procedures. Neuropsychopharmacology 14, 375–424. [PubMed: 8726752]

Muller PA, Schneeberger M, Matheis F, Wang P, Kerner Z, Ilanges A, Pellegrino K, Del Marmol J, Castro TBR, Furuichi M, Perkins M, Han W, Rao A, Pickard AJ, Cross JR, Honda K, de Araujo I, Mucida D, 2020. Microbiota modulate sympathetic neurons via a gut-brain circuit. Nature 583, 441–446. [PubMed: 32641826]

Needham BD, Funabashi M, Adame MD, Wang Z, Boktor JC, Haney J, Wu WL, Rabut C, Ladinsky MS, Hwang SJ, Guo Y, Zhu Q, Griffiths JA, Knight R, Bjorkman PJ, Shapiro MG, Geschwind DH, Holschneider DP, Fischbach MA, Mazmanian SK, 2022. A gut-derived metabolite alters brain activity and anxiety behaviour in mice. Nature 602, 647–653. [PubMed: 35165440]

Neufeld KM, Kang N, Bienenstock J, Foster JA, 2011. Reduced anxiety-like behavior and central neurochemical change in germ-free mice. Neuro Gastroenterol. Motil. 23, 255–264 e119.

O'Connor RM, Moloney RD, Glennon J, Vlachou S, Cryan JF, 2015. Enhancing glutamatergic transmission during adolescence reverses early-life stress-induced deficits in the rewarding effects of cocaine in rats. Neuropharmacology 99, 168–176. [PubMed: 26187394]

O'Donnell MP, Fox BW, Chao PH, Schroeder FC, Sengupta P, 2020. A neurotransmitter produced by gut bacteria modulates host sensory behaviour. Nature 583, 415–420. [PubMed: 32555456]

Paul J McMurdie SH, 2014. Waste not, want not: why rarefying microbiome data is inadmissible. PLoS Comput. Biol. 10, 12.

Peterson VL, Richards JB, Meyer PJ, Cabrera-Rubio R, Tripi JA, King CP, Polesskaya O, Baud A, Chitre AS, Bastiaanssen TFS, Woods LS, Crispie F, Dinan TG, Cotter PD, Palmer AA, Cryan JF, 2020. Sex-dependent associations between addiction-related behaviors and the microbiome in outbred rats. EBioMedicine 55, 102769. [PubMed: 32403084]

Reyes REN, Al Omran AJ, Davies DL, Asatryan L, 2020. Antibiotic-induced disruption of commensal microbiome linked to increases in binge-like ethanol consumption behavior. Brain Res. 1747, 147067. [PubMed: 32827548]

Reyes RE, Gao L, Zhang Z, Davies DL, Asatryan L, 2022. Supplementation with sodium butyrate protects against antibiotic-induced increases in ethanol consumption behavior in mice. Alcohol 100, 1–9. [PubMed: 34999234]

Robert C Edgar BJH, Clemente Jose C., Quince Christopher, Knight Rob, 2011. UCHIME improves sensitivity and speed of chimera detection. Bioinformatics 27, 2194–2200. [PubMed: 21700674]

Roberts AJ, Casal L, Huitron-Resendiz S, Thompson T, Tarantino LM, 2018. Intravenous cocaine self-administration in a panel of inbred mouse strains differing in acute locomotor sensitivity to cocaine. Psychopharmacology (Berl) 235, 1179–1189. [PubMed: 29423710]

Saul MC, Philip VM, Reinholdt LG, Center for Systems Neurogenetics of A, Chesler EJ, 2019. High-diversity mouse populations for complex traits. Trends Genet. 35, 501–514. [PubMed: 31133439]

Schoenrock SA, Kumar P, Gomez AA, Dickson PE, Kim SM, Bailey L, Neira S, Riker KD, Farrington J, Gaines CH, Khan S, Wilcox TD, Roy TA, Leonardo MR, Olson AA, Gagnon LH, Philip VM, Valdar W, de Villena FP, Jentsch JD, Logan RW, McClung CA, Robinson DL, Chesler EJ, Tarantino LM, 2020. Characterization of genetically complex Collaborative Cross mouse strains that model divergent locomotor activating and reinforcing properties of cocaine. Psychopharmacology (Berl) 237, 979–996. [PubMed: 31897574]

Shiraki T, Koshimura K, Kobayashi S, Miwa S, Masaki T, Watanabe Y, Murakami Y, Kato Y, 1996. Stimulating effect of 6R-tetrahydrobiopterin on Ca2+ channels in neurons of rat dorsal motor nucleus of the vagus. Biochem. Biophys. Res. Commun. 221, 181–185. [PubMed: 8660332]

Shreiner AB, Kao JY, Young VB, 2015. The gut microbiome in health and in disease. Curr. Opin. Gastroenterol. 31, 69–75. [PubMed: 25394236]

Stewart Campbell A, Needham BD, Meyer CR, Tan J, Conrad M, Preston GM, Bolognani F, Rao SG, Heussler H, Griffith R, Guastella AJ, Janes AC, Frederick B, Donabedian DH, Mazmanian SK, 2022. Safety and target engagement of an oral small-molecule sequestrant in adolescents with autism spectrum disorder: an open-label phase 1b/2a trial. Nat. Med. 28, 528–534. [PubMed: 35165451]

Sukoff Rizzo SJ, Crawley JN, 2017. Behavioral phenotyping assays for genetic mouse models of neurodevelopmental, neurodegenerative, and psychiatric disorders. Annu Rev Anim Biosci 5, 371–389. [PubMed: 28199172]

Svenson KL, Gatti DM, Valdar W, Welsh CE, Cheng R, Chesler EJ, Palmer AA, McMillan L, Churchill GA, 2012. High-resolution genetic mapping using the Mouse Diversity outbred population. Genetics 190, 437–447. [PubMed: 22345611]

Threadgill DW, Churchill GA, 2012. Ten years of the collaborative cross. G3 (Bethesda) 2, 153–156. [PubMed: 22384393]

Valles-Colomer M, Falony G, Darzi Y, Tigchelaar EF, Wang J, Tito RY, Schiweck C, Kurilshikov A, Joossens M, Wijmenga C, Claes S, Van Oudenhove L, Zhernakova A, Vieira-Silva S, Raes J, 2019. The neuroactive potential of the human gut microbiota in quality of life and depression. Nat Microbiol 4, 623–632. [PubMed: 30718848]

Volpe GE, Ward H, Mwamburi M, Dinh D, Bhalchandra S, Wanke C, Kane AV, 2014. Associations of cocaine use and HIV infection with the intestinal microbiota, microbial translocation, and inflammation. J. Stud. Alcohol Drugs 75, 347–357. [PubMed: 24650829]

Walker MA, Pedamallu CS, Ojesina AI, Bullman S, Sharpe T, Whelan CW, Meyerson M, 2018. GATK PathSeq: a customizable computational tool for the discovery and identification of microbial sequences in libraries from eukaryotic hosts. Bioinformatics 34, 4287–4289. [PubMed: 29982281]

Weiss S, Xu ZZ, Peddada S, Amir A, Bittinger K, Gonzalez A, Lozupone C, Zaneveld JR, Vazquez-Baeza Y, Birmingham A, Hyde ER, Knight R, 2017. Normalization and microbial differential abundance strategies depend upon data characteristics. Microbiome 5, 27. [PubMed: 28253908]

Wickham H, 2016. ggplot2 : Elegant Graphics for Data Analysis. Use R! Springer International Publishing : Imprint: Springer, Cham, p. 1 online resource (XVI, 260 pages 232 illustrations, 140 illustrations in color.

Yang J, Zheng P, Li Y, Wu J, Tan X, Zhou J, Sun Z, Chen X, Zhang G, Zhang H, Huang Y, Chai T, Duan J, Liang W, Yin B, Lai J, Huang T, Du Y, Zhang P, Jiang J, Xi C, Wu L, Lu J, Mou T, Xu Y, Perry SW, Wong ML, Licinio J, Hu S, Wang G, Xie P, 2020. Landscapes of bacterial and metabolic signatures and their interaction in major depressive disorders. Sci. Adv. 6.

Yano JM, Yu K, Donaldson GP, Shastri GG, Ann P, Ma L, Nagler CR, Ismagilov RF, Mazmanian SK, Hsiao EY, 2015. Indigenous bacteria from the gut microbiota regulate host serotonin biosynthesis. Cell 161, 264–276. [PubMed: 25860609]

Zheng P, Zeng B, Liu M, Chen J, Pan J, Han Y, Liu Y, Cheng K, Zhou C, Wang H, Zhou X, Gui S, Perry SW, Wong ML, Licinio J, Wei H, Xie P, 2019. The gut microbiome from patients with schizophrenia modulates the glutamate-glutamine-GABA cycle and schizophrenia-relevant behaviors in mice. Sci. Adv. 5, eaau8317. [PubMed: 30775438]

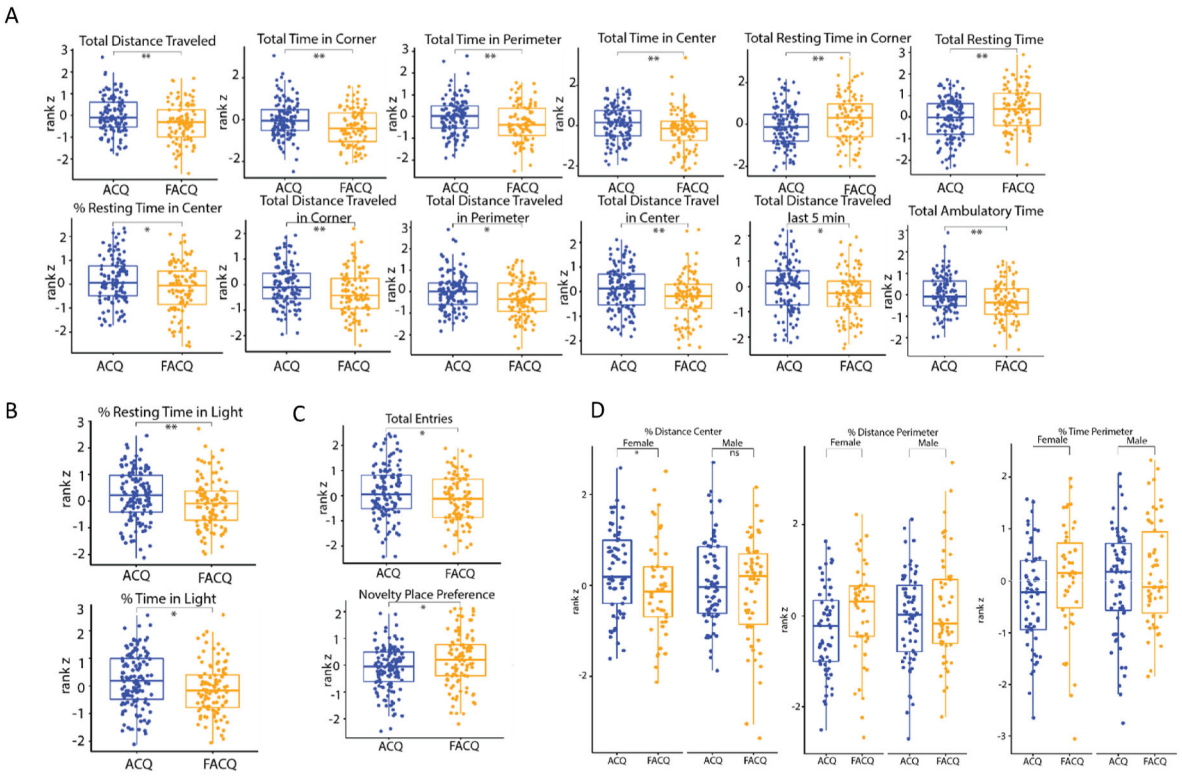

Fig. 1.

Novelty behaviors are associated with the acquisition of IVSA. A) The twelve open field measures that differed between ACQ and FACQ. From top left to lower right. Total distance traveled, total time in corner, total time in perimeter, total time in center, total resting time in corner, total resting time, percent resting time in center, total distance traveled in corner, toral distance traveled in the perimeter, total distance traveled in the center, the total distance traveled in the last 5 min and the total ambulatory time. B) The two light-dark metrics that differed between ACQ and FACQ, the percent resting time in the light and the percent time in the light C) The hole board total entries and the preference for a novel arena differed between ACQ and FACQ mice. D) Sex specificity of novelty behaviors associated with the acquisition of IVSA. Three open field measures were significantly different in females, the distance time (as a percent) in the center, and, the percent distance and time in the perimeter. ACQ is in blue and FACQ is in orange. Outliers have been removed from the phenotype data, and the values rank z transformed. *$p < 0.05$, **$p < 0.01$.

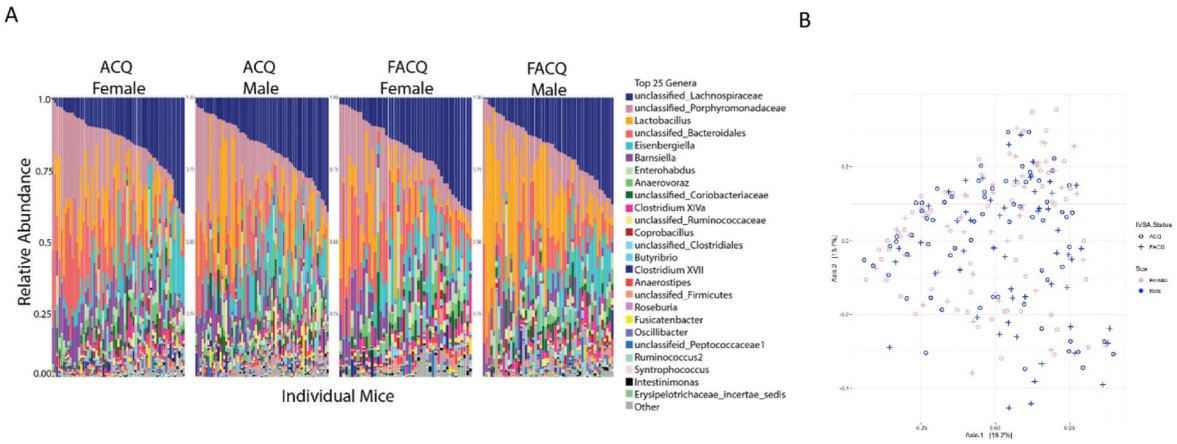

Fig. 2.

Microbial composition of the ACQ vs. FACQ groups of DO mice. A) The percent abundance of the 25 most abundant genera in female and male mice ACQ and FACQ mice. B) Principal components analysis of bacterial beta diversity at OTU level using Bray-Curtis for 16 S microbiome data showing the ACQ, FACQ, and male and female groupings.

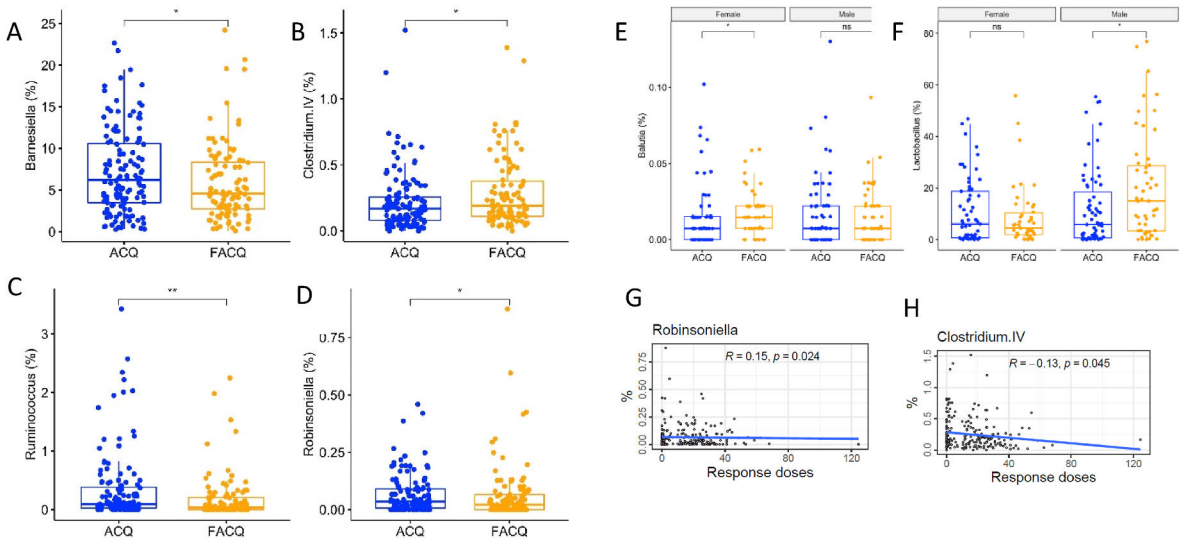

Fig. 3.

Differential gut microbiome composition of ACQ and FACQ mice. A) *Barnesiella, B) Clostridium* IV, C) *Ruminococcus*, D) *Robinsoniella,* E) Sex-dependent associations *of Blautia and F) Lactobacillus.* G) Correlation between *Robinsoniella abundance* and doses of cocaine administered during the acquisition phase. H) Correlation between *Clostridium* IV abundance and doses of cocaine administered during the acquisition phase.

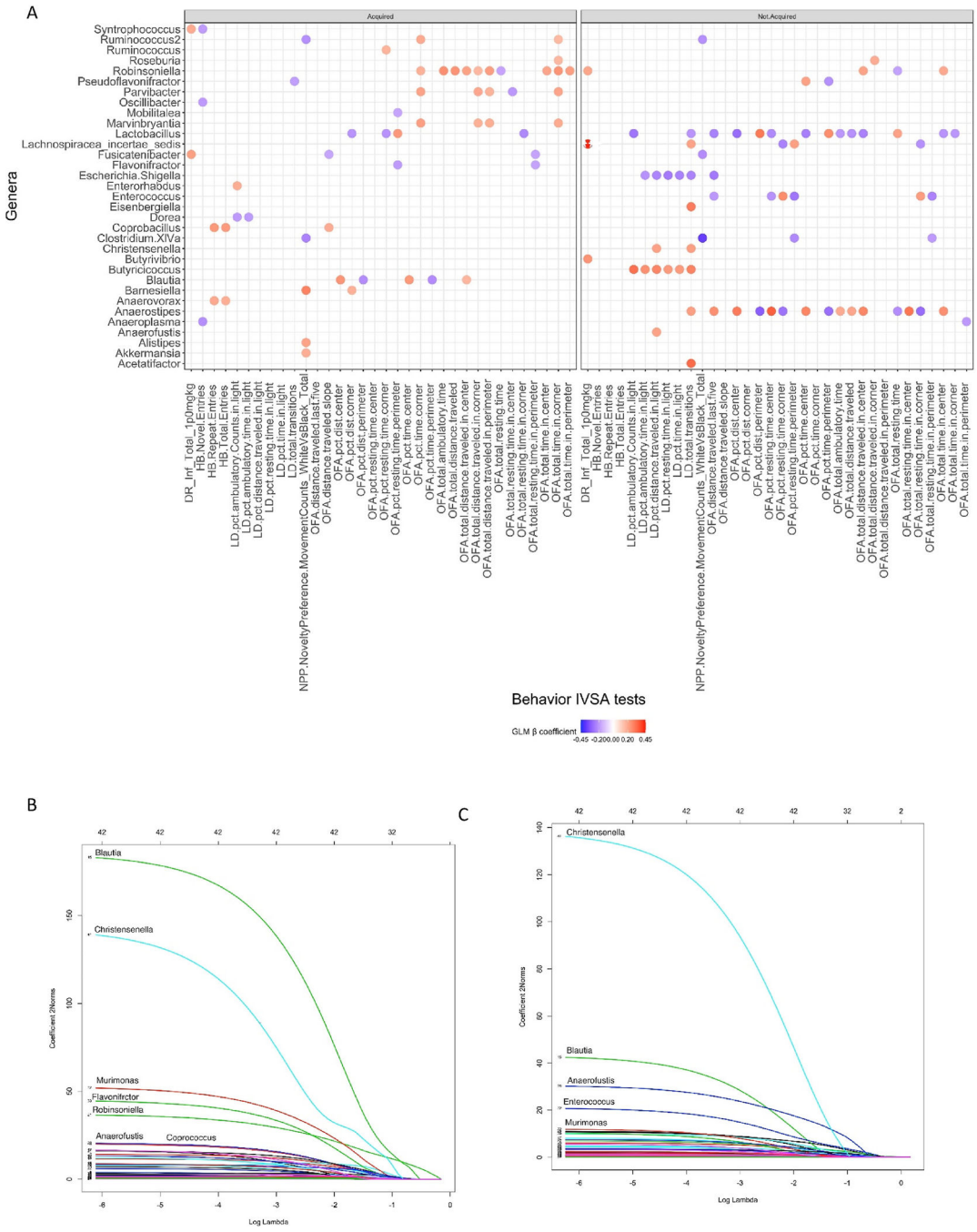

Fig. 4.

Novelty behaviors associated with microbial abundance in the DO mice A. Generalized linear model results for specific effects of the microbiome on behavior in DO mice. The GLM fit was $Behavior_i \sim Age + Sex + Genus_j$ B) Lasso regression analysis of the microbiomes as predictors of behavior.

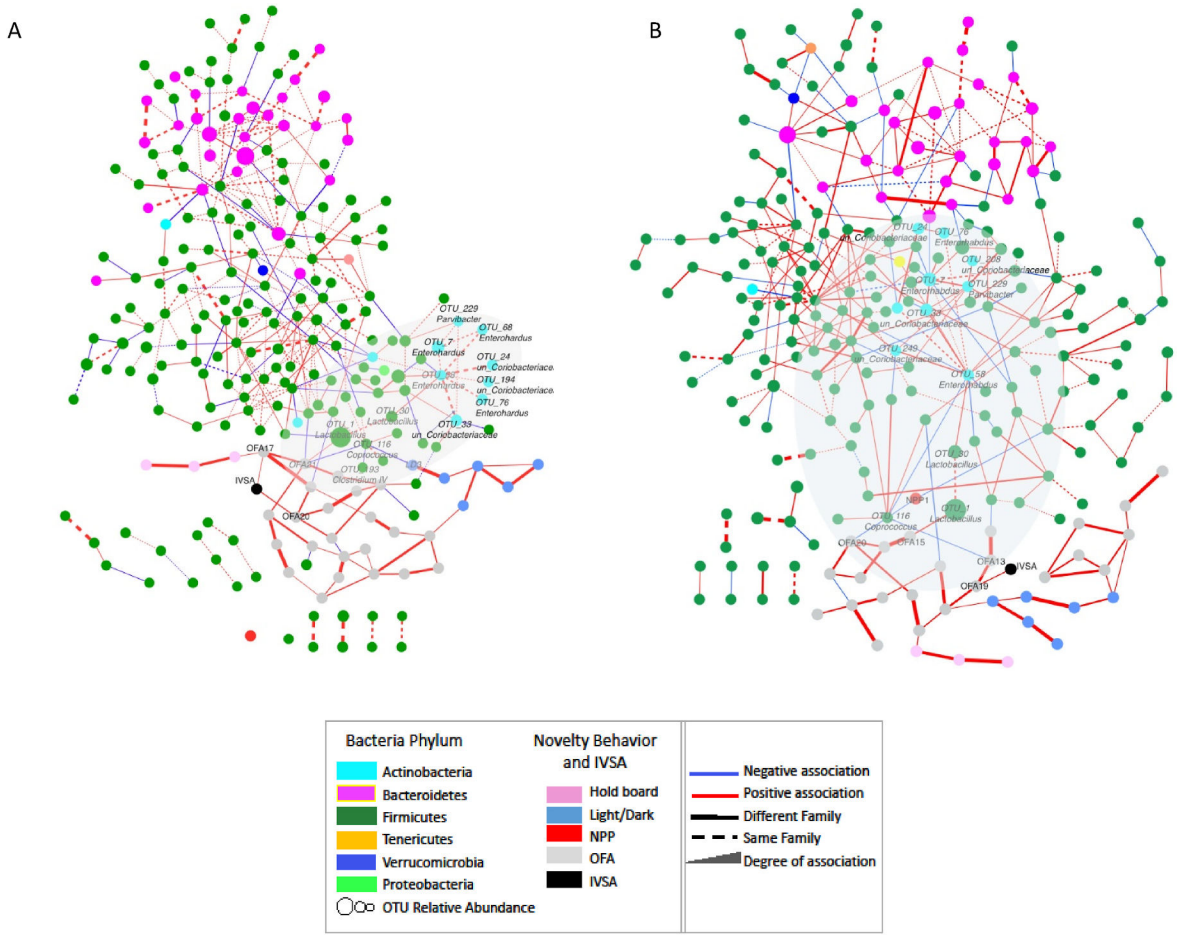

Fig. 5.

Network analysis of ACQ and FACQ at OTU level: interactions between microbe-microbe and microbe-behavior. The network was built on filtered 50% OTU prevalence of DO mice cohort using SPIEC-EASI. Each OTU and each novelty behavior was considered as a node in the network. Abbreviations in network: novelty place preference (NPP1), percent distance in the center (OFA13), percent distance in the perimeter (OFA15), percent time in the corner (OFA17), percent resting time in the center (OFA19), percent resting time in the corner (OFA20), percent resting time in the perimeter (OFA21), percent resting time in the light (LD3), Number of infusions at 1.0 mg/kg (IVSA).

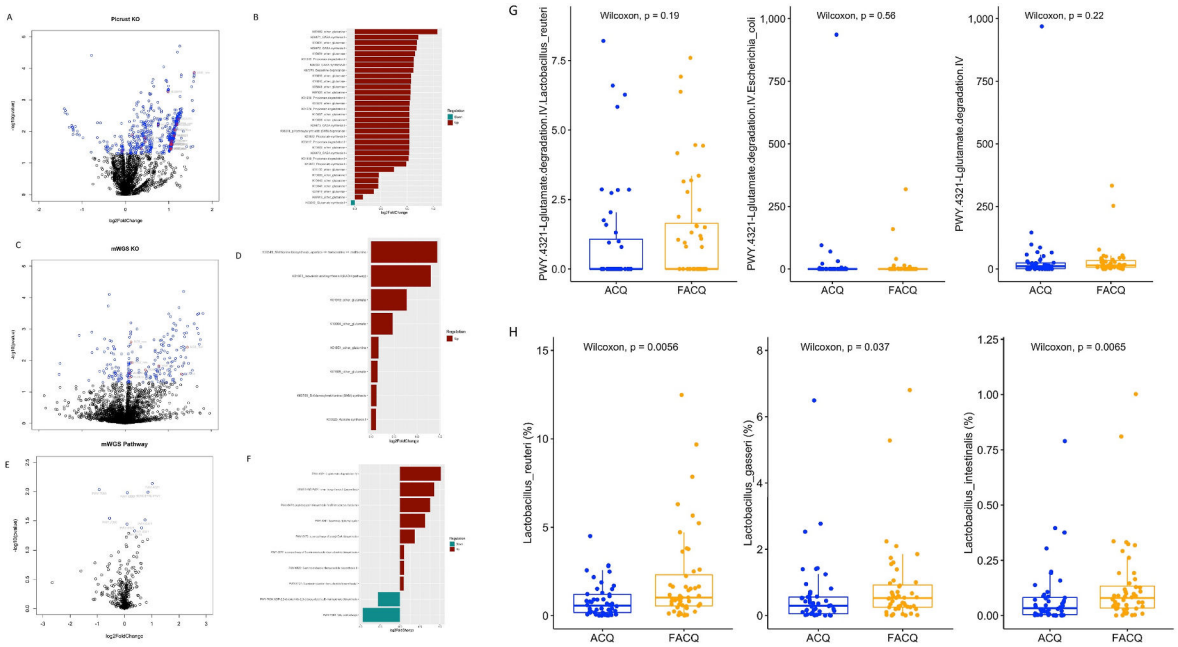

Fig. 6.

Volcano plots of the functional categories encoded by the microbiome. A. A scatterplot showing the statistical significance and magnitude of change of the KO clusters as determined by PICRUSt2 of 16S data. B. The KO categories ($p < 0.05$) from PICRUSt2 of 16S data. C. A scatterplot of the statistical significance and magnitude of change of the KO clusters determined by mWGS. D. The KO categories ($p < 0.05$) from mWGS data. E. A scatterplot of the statistical significance and magnitude of change of the mWGS Pathways F. The mWGS Pathways ($p < 0.05$) blue = significant KO/pathway (p value < 0.05), red = significant KOs that are GBM (p value < 0.05). G. H.

Neuropharmacology. Author manuscript; available in PMC 2023 March 15.

Tables 1

16S metabolic potential analysis.

id	baseMean	log 2 FoldChange	lfcSE	stat	pvalue	QVALUE	GBM_ID	GBM_NAME	KO.picrust.description
K00982	4.70	1.58	0.42	3.81	0.00014	0.01797994	MGB_new	other_glutamine	glnE; [glutamine synthetase] adenylyltransferase/[glutamine synthetase]-adenylyl-L-tyrosine phosphorylase [EC:2.7.7.42 2.7.7.89]
K13923	186.18	0.99	0.29	3.45	0.00055	0.03620277	MGB048	Propionate synthesis I	pduL; phosphate propanoyltransferase [EC:2.3.1.222]
K09471	4.14	1.22	0.42	2.88	0.00404	0.13505818	MGB020	GABA synthesis I	puuB, ordL; gamma-glutamylputrescine oxidase [EC:1.4.3.-]
K10001	4.15	1.19	0.43	2.77	0.00558	0.13505818	MGB_new	other_glutamate	gltI, aatJ; glutamate/aspartate transport system substratebinding protein
K11102	210.37	0.75	0.27	2.74	0.00617	0.13505818	MGB_new	other_glutamate	gltP, gltT; proton glutamate symport protein
K09472	3.58	1.18	0.43	2.74	0.00621	0.13505818	MGB020	GABA synthesis I	puuC, aldH; 4-(gamma-glutamylamino)butanal dehydrogenase [EC:1.2.1.99]
K01682	3.59	1.13	0.43	2.62	0.00877	0.14779758	MGB056	Propionate degradation I	acnB; aconitate hydratase 2/2-methylisocitrate dehydratase [EC:4.2.1.3 4.2.1.99]
K10004	3.29	1.15	0.44	2.61	0.00906	0.14779758	MGB_new	other_glutamate	gltL, aatP; glutamate/aspartate transport system ATP-binding protein [EC:3.6.3.-]
K07010	20409.07	0.16	0.06	2.49	0.01272	0.15273522	MGB_new	other_glutamine	K07010; putative glutamine amidotransferase
K00276	3.17	1.12	0.45	2.47	0.01335	0.15273522	MGB023	Dopamine degradation	AOC3, AOC2, tynA; primary-amine oxidase [EC:1.4.3.21]
K00137	3.18	1.12	0.46	2.46	0.01381	0.15273522	MGB021	GABA synthesis II	prr; aminobutyraldehyde dehydrogenase [EC:1.2.1.19]
K10041	3512.34	0.45	0.19	2.41	0.01575	0.15273522	MGB_new	other_glutamine	ABC.GLN1.A; putative glutamine transport system ATP-binding protein [EC:3.6.3.-]
K10040	6999.89	0.45	0.19	2.41	0.01595	0.15273522	MGB_new	other_glutamine	ABC.GLN1.P; putative glutamine transport system permease protein
K07320	3.20	1.07	0.46	2.34	0.01950	0.15273522	MGB_new	other_glutamine	prmB; ribosomal protein L3 glutamine methyltransferase [EC:2.1.1.298]
K01908	3.19	1.06	0.46	2.32	0.02054	0.15273522	MGB056	Propionate degradation I	prpE; propionyl-CoA synthetase [EC:6.2.1.17]
K10039	5621.62	0.46	0.20	2.30	0.02161	0.15273522	MGB_new	other_glutamine	ABC.GLN1.S; putative glutamine transport system substrate-binding protein
K03417	3.10	1.04	0.46	2.25	0.02439	0.15273522	MGB056	Propionate degradation I	prpB; methylisocitrate lyase [EC:4.1.3.30]
K10002	3.04	1.08	0.48	2.25	0.02466	0.15273522	MGB_new	other_glutamate	gltK, aatM; glutamate/aspartate transport system permease protein
K10003	3.04	1.08	0.48	2.25	0.02466	0.15273522	MGB_new	other_glutamate	gltJ, aatQ; glutamate/aspartate transport system permease protein
K06048	3.03	1.07	0.48	2.23	0.02562	0.15273522	MGB_new	other_glutamate	gshA, ybdK; glutamate—cysteine ligase/carboxylate-amine ligase [EC:6.3.2.2 6.3.-.-]
K01659	3.11	1.03	0.46	2.23	0.02574	0.15273522	MGB056	Propionate degradation I	prpC; 2-methylcitrate synthase [EC:2.3.3.5]

id	baseMean	log 2 FoldChange	lfcSE	stat	pvalue	QVALUE	GBM_ID	GBM_NAME	KO.picrust.description
K01720	3.08	1.05	0.47	2.22	0.02613	0.15273522	MGB056	Propionate degradation I	prpD; 2-methylcitrate dehydratase [EC:4.2.1.79]
K01919	**2394.20**	**0.36**	**0.17**	**2.12**	**0.03384**	**0.15273522**	**MGB_new**	**other_glutamate**	**gshA; glutamate-cysteine ligase [EC:6.3.2.2]**
K05526	2.93	1.05	0.50	2.11	0.03450	0.15273522	MGB_new	other_glutamate	astE; succinylglutamate desuccinylase [EC:3.5.1.96]
K09470	2.92	1.04	0.49	2.11	0.03501	0.15273522	MGB020	GABA synthesis I	puuA; gamma-glutamylputrescine synthase [EC:6.3.1.11]
K10036	2.92	1.04	0.50	2.10	0.03577	0.15273522	MGB_new	other_glutamine	glnH; glutamine transport system substratebinding protein
K10037	2.92	1.04	0.50	2.10	0.03577	0.15273522	MGB_new	other_glutamine	glnP; glutamine transport system permease protein
K09473	2.92	1.04	0.50	2.10	0.03577	0.15273522	MGB020	GABA synthesis I	puuD; gamma-glutamyl-gamma-aminobutyrate hydrolase [EC:3.5.1.94]
K08318	2.92	1.04	0.50	2.10	0.03577	0.15273522	MGB039	g-Hydroxybutyric acid (GHB) degradation	yihU; 4-hydroxybutyrate dehydrogenase/sulfolactaldehyde 3-reductase [EC:1.1.1.61 1.1.1.373]
K00932	2.92	1.04	0.50	2.10	0.03577	0.15273522	MGB048	Propionate synthesis I	tdcD; propionate kinase [EC:2.7.2.15]
K10038	2.92	1.04	0.50	2.09	0.03628	0.15273522	MGB_new	other_glutamine	glnQ; glutamine transport system ATP-binding protein [EC:3.6.3.-]
K00262	33757.40	−0.07	0.04	−2.04	0.04156	0.1695214	MGB006	Glutamate synthesis I	E1.4.1.4, gdhA; glutamate dehydrogenase (NADP+) [EC:1.4.1.4]

Table 2

WGS metabolic potential analysis.

id	baseMean	log 2 FoldChange	lfcSE	stat	pvalue	qvalue	GBM_ID	GBM_NAME	KO.name
K01928	277.38	0.14	0.05	3.01	0.00259	0.25929	MGB_new	other_glutamate	K01928: UDP-*N*-acetylmuramoylalanyl-D-glutamate-2,6-diaminopimelate ligase [EC:6.3.2.13]
K00549	6.58	1.44	0.50	2.90	0.00379	0.25929	MGB_new	Methionine biosynthesis, apartate => homoserine => methionine	K00549: 5-methyltetrahydropteroyltrigluta-mate-homocysteine methyltransferase [EC:2.1.1.14]
K01951	321.30	0.16	0.06	2.52	0.01169	0.51059	MGB_new	other_glutamine	K01951: GMP synthase (glutamine-hydrolysing) [EC:6.3.5.2]
K01919	14.12	0.78	0.32	2.43	0.01491	0.51059	MGB_new	other_glutamate	K01919: glutamate-cysteine ligase [EC:6.3.2.2]
K10004	46.86	0.47	0.20	2.33	0.01999	0.52988	MGB_new	other_glutamate	K10004: glutamate/aspartate transport system ATP-binding protein [EC:3.6.3.-]
K00625	252.35	0.11	0.05	2.23	0.02543	0.52988	MGB043	Acetate synthesis I	K00625: phosphate acetyltransferase [EC:2.3.1.8]
K01073	2.35	1.30	0.59	2.21	0.02707	0.52988	MGB034	Isovaleric acid synthesis I (KADH pathway)	K01073: acyl-CoA hydrolase [EC:3.1.2.20]
K00789	488.20	0.11	0.05	2.12	0.03433	0.58795	MGB036	*S*-Adenosylmethionine (SAM) synthesis	K00789: *S*-adenosylmethionine synthetase [EC:2.5.1.6]

Table 3

WGS pathway analysis.

baseMean	log 2 Fold Change	lfcSE	stat	pvalue	padj	id	description
15.17	1.02	0.38	2.68	0.00725777473658956	0.928134468622901	PWY.4321	PWY-4321: L-glutamate degradation IV
26.10	−0.93	0.36	−2.60	0.00923576062316964	0.928134468622901	PWY.7094	PWY-7094: fatty acid salvage
14.18	0.86	0.33	2.57	0.0101900274459023	0.928134468622901	HEMESYN2.PWY	HEMESYN2-PWY: heme biosynthesis II (anaerobic)
461.86	0.10	0.04	2.56	0.0104284771755382	0.928134468622901	PWY.6122	PWY-6122: 5-aminoimidazole ribonucleotide biosynthesis II
461.86	0.10	0.04	2.56	0.0104284771755382	0.928134468622901	PWY.6277	PWY-6277: superpathway of 5-aminoimidazole ribonucleotide biosynthesis
736454.01	0.08	0.03	2.44	0.0148825655837792	0.997609979621882	UNMAPPED	UNMAPPED
582392.85	−0.08	0.03	−2.31	0.0208788630382158	0.997609979621882	UNINTEGRATED	UNINTEGRATED
2.11	−0.55	0.25	−2.19	0.0287208034366106	0.997609979621882	PWY.7090	PWY-7090: UDP-2,3-diacetamido-2,3-dideoxy-α-D-mannuronate biosynthesis
51.73	0.75	0.35	2.16	0.0305712722129547	0.997609979621882	PWY.6471	PWY-6471: peptidoglycan biosynthesis IV (Enterococcus faecium)
428.35	0.09	0.04	2.10	0.0358942214852572	0.997609979621882	PWY.6121	PWY-6121: 5-aminoimidazole ribonucleotide biosynthesis I
29.42	0.63	0.31	2.04	0.0415726257765415	0.997609979621882	PWY.4041	PWY-4041: γ-glutamyl cycle
21.53	0.37	0.19	1.99	0.0469795143047049	0.997609979621882	PWY.5173	PWY-5173: superpathway of acetyl-CoA biosynthesis